Coordination Chemistry Reviews, 39 (1981) 181–224
Elsevier Scientific Publishing Company, Amsterdam—Printed in The Netherlands

THE MECHANISMS OF PHOTOREACTIVITY OF COORDINATION COMPOUNDS: LIMITING CASES OF DECAY ON A SPECIFIC NUCLEAR COORDINATE (DOSENCO) OR VIA RANDOM COORDINATE SELECTION (DERCOS)

BRYAN R. HOLLEBONE and COOPER H. LANGFORD *

Metal Ions Group, Chemistry Department, Carleton University, Ottawa K1S 5B6 (Canada)

NICK SERPONE

Department of Chemistry, Concordia University, Montreal, Quebec H3G 1M8 (Canada)

(First received 23 September 1980; in revised form 19 March 1981)

CONTENTS

---

* Correspondence to this author should now be addressed to Department of Chemistry, Concordia University, Montreal H3G 1M8, Canada.

A. INTRODUCTION: TWO LIMITING CASES OF EXCITED STATE DECAY

This review concerns the detailed mechanisms of photoreactions in transition metal complexes. By this is meant the analysis of events following the initial population of the excited state responsible for the reaction. Two approaches have appeared in the literature. One could be called a photochemical model and the other photophysical [1]. These terms will not be retained because they have other uses which could lead to ambiguity but they will be useful initially in defining the issues.

Photochemical theories [2–4] are those that employ many of the ideas developed in the extensive literature of thermal kinetics. They invoke concepts of structure-reactivity correlations such as the Marcus theory which connects $\Delta G^{\ddagger}$ to ΔG^{0} and descriptions of chemical events in terms of nucleophilicity or associative substitution. Implicitly or explicitly these concepts all use transition state theory. This theory is based on a pseudo-equilibrium assumption of a Boltzmann distribution over all molecular degrees of freedom. Adamson et al. [5,6] have identified this condition as a thermally equilibrated excited state (thexi). These states may be regarded as little more than electronic isomers of ground states and there is little reason to abandon the concepts of transition state theory.

Reaction rates at the photochemical limit depend inversely on the energy barriers of each decay channel. The selection of a particular mechanism is governed by the random distribution of normal modes at the effective Boltzmann temperature. From this mechanistic point of view, the events following the initial population of the thexi state can be identified as decay by random coordinate selection. This will be identified as the DERCOS limit mechanism. The model has proven to be very useful in many systems. To document this we will outline the uses of Marcus theory for metal complex photochemistry in Section B(ii) and review examples of DERCOS photosubstitution in Section B(iii).

Hammond has remarked [7] that the dissipation of the large localized quantity of energy derived from the absorbed photon must be kept clearly in mind. It is the driving force for photoreaction. Hammond's point has two important implications. First, it means that reactions treated within transition state theory, the DERCOS limit, will be subject to a constraint that is not general in thermal chemistry. They will all tend to be exothermic. We discuss the consequences in Section B(i). Secondly, this point suggests the possibility that the dissipation of excess energy could initiate irreversible radiationless processes before vibrational equilibrium is established. These alternative processes could occur in competition with vibrational relaxation of the electronic excited state and be too rapid for analysis under the assumptions of the DERCOS limit.

Initially this is an empirical question. The evidence that such processes are important in transition metal photochemistry is reviewed in Section C. The available indications that some of these reactions do occur at such a photophysical limit [1], focus attention on the development of theories of fast reactions based on the electronic structures of transition metal complexes. In such models, the tendency towards selection of reaction channels is predicted from spectroscopic data. The most advanced predictions of this type are those of Vanquickenborne and Ceulemans [8–10].

In the photophysical limit the usefulness of these theories is marginal, however, since the role of inter- and intramolecular dynamic processes is neglected. The omission of these effects is easily understood for, in conventional form, the structure and solutions of the differential equations used to describe radiationless processes are formidable even in small molecules [11]. However, these conventional solutions are obtained using some inappropriate assumptions and neglecting the surprisingly simple algebra associated with the vectorial behaviour of the wave functions.

Some initial approaches have been made towards analysis of the vectorial algebra and the derivation of electronic selection rules for reactions from that algebra. This initiative is reviewed in Section D(i). Very recently, a vectorial technique incorporating both electronic and dynamic molecular structure has been developed [1,12], which provides simple but powerful selection rules for prediction of fast reaction coordinates. The fundamental assumption in this model is that fast reactions occur under conditions of strong vibronic coupling. In this limit, the electronic excitation energy can rapidly be converted into pathological nuclear motion. Thus, the Born–Oppenheimer assumption of weak coupling, which may be appropriate in the DERCOS limit, is abandoned. Instead, the rates of fast reactions are described in Section D(ii) in terms of the symmetry and intensity of time-dependent perturbations which permit transitions between vibronic states. Under these conditions, the selection rules identify processes of decay on selected nuclear coordinates (DOSENCO) which are strongly allowed in comparison to other processes which remain forbidden at the chosen order of approximation [12]. Empirical consequences of the analysis are sought in Section D(iii).

These selection rule techniques appear to provide an appropriate complement, in the limit of fast reactions, to the transition state model in the limit of vibrational equilibrium. When decay of photoexcited states is slow, it can be assumed that first-order processes are forbidden and only those decay events associated with higher-order perturbations are available. In these cases a full analysis using selection rules would be difficult and an analysis with transition state theory is a simple, valid alternative. In systems in which first-order perturbations are allowed and equilibrium is not achieved, the transition state theory will fail. The simplest analysis is then treatment as a DOSENCO state.

Sufficient evidence is now available to suggest the need for different models for slow and fast photoreaction mechanisms. Thus we wish to employ the two complementary models of photoreactions, one based on an appropriate extension of transition state theory and the other on strongly coupled vibronic systems. Each of these provides an adequate account of both the electronic and atomic dynamics in the two limiting time domains.

B. DECAY VIA RANDOM COORDINATE SELECTION (DERCOS) MECHANISMS

(i) General considerations

In the case that an excited state from which a reaction originates is long-lived, the steps requiring elucidation include at least the following: (a) the excitation process; (b) any intersystem crossing; (c) vibrational and orientational relaxation within the spin manifold of the reactive random state; (d) the photoreaction step; and (e) internal conversion to the ground state in competition with reaction. (Luminescence processes may also be included without difficulty and will be omitted for now.) The minimal steps are summarized in eqn. (1).

$$\begin{tikzcd}
A \arrow[r] \arrow[rr, bend right, "k_1"'] & {}^*A_n \arrow[r] & {}^*A_0 \arrow[r, "k_{rxn}"] \arrow[ll, bend right, "k_{-1}"'] & B
\end{tikzcd} \tag{1}$$

In this equation, A represents the ground state, ${}^*A_n$ is the rovibrationally excited Franck–Condon state and ${}^*A_0$ is the DERCOS state decaying by thermalized random selection of the available pathways. (This equation assumes for simplicity that only one electronic excited state is important.) k_1 is the rate constant for production of the excited thexi state, ${}^*A_0$. It combines a constant for a "photophysical" relaxation process with absorption. k_{-1} is the rate constant for return to the ground state. This may be a process with features in common with the reaction since it occurs in competition unless the reaction quantum yield is either unity or very small. Thus, k_{-1} may, like the product formation rate constant, be subject to analysis with the aid of chemical kinetic concepts. k_{rxn} is the rate constant for the formation of the photoproduct B. It is the rate constant on which we shall focus first. We return to k_{-1} later.

An example from the very recent literature [13] can make ideas concrete. It concerns the reaction described in eqn. (2).

$$\mathrm{Rh(NH_3)_5Cl^{2+} + H_2O \xrightarrow{h\nu} Rh(NH_3)_5OH_2^{3+} + Cl^-} \tag{2}$$

The specially useful feature of this reaction is that temperature dependence was measured and luminescence allows for placement of the DERCOS state on an energy axis. Consequently, the qualitative energy diagram in Fig. 1 can be drawn for this reaction.

The overall reaction is only mildly exergonic in aqueous media. The photon required to excite the complex is quite large by comparison. Emission and excited state absorption were studied using a pulsed Nd-glass laser [13]. Emission was centred at 640 nm which corresponds to an energy of 188 kJ mol^{-1} (45 kcal mol^{-1}). This is, for example, much larger than the activation energy for thermal substitution. The activation energy associated with decay of the emitting excited state is 22.6 kJ mol^{-1} (5.4 kcal mol^{-1}). Thus, a reaction coordinate diagram comparing thermal and photochemical substitution is qualitatively represented in Fig. 1 (the photoreaction is a DERCOS state reaction). Note that the thermal transition state differs greatly in energy from both the reactant and the product. In contrast, the photoreaction from the DERCOS state is, in common with most photoreactions, highly exergonic. Since the barrier for decay of this state is only 22.6 kJ mol^{-1} (5.4 kcal mol^{-1}), it is probable that the DERCOS state does not

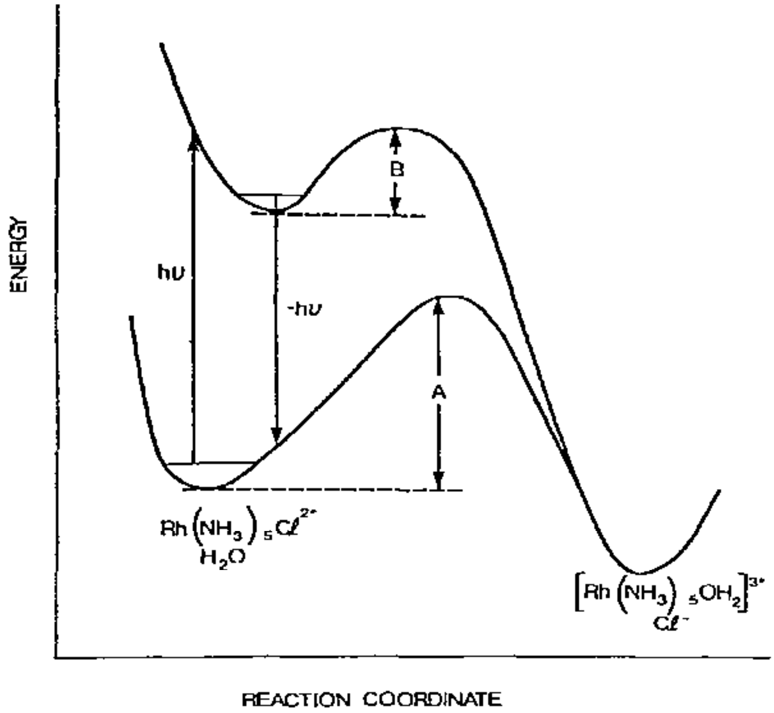

Fig. 1. Qualitative energy diagram comparing thermal and photochemical substitution.

differer greatly from the transition state for formation of the photoproduct.

A very useful principle in thermal kinetics, Hammond's postulate [14], can be applied to the appreciation of the situation:

> If two states (as, for example, a transition state and an unstable intermediate) occur consecutively during a reaction process and have nearly the same energy content, their interconversion will require only a small reorganization of molecular structure.

Hammond's postulate has often been used to argue that highly exergonic reactions have transition states similar to the initial states. Hammond's idea leads to the conclusion that photoreaction transition states commonly resemble DERCOS states in structure as a consequence of the similarity in energy.

The result emerging from analysis of DERCOS state reactivity using Hammond's postulate is quite important. It reveals that DERCOS states will tend not to show high selectivity. If the transition state is close to the DERCOS state, there is very little room for variation in the energy difference marked *B* in Fig. 1 (contrast the energy difference marked *A* for the thermal reaction). Thermal reactions can be highly chemically selective as a result of the variation in energy difference between the ground state and transition state as structure is varied. Because of the consistently exothermic behaviour of DERCOS states, such selectivity as a function of structure-reactivity relationships will be compressed in most cases.

If the preceding point is correct, then it is fair to conclude that the differences in reactivity among various structures (the stuff of structure-reactivity relations) will be largely determined by the structures and energies of the DERCOS states themselves. Put alternatively, the consequence of application of Hammond's postulate is the conclusion that DERCOS states are usually well prepared for reaction. This idea is not foreign to photochemists. The present analysis simply integrates it to transition state theory.

The considerations just introduced suggest that structure-reactivity correlations for overall photoreaction will closely map changes in the DERCOS state. Thus, continued study of DERCOS states is of considerable importance [5].

The conclusion that photochemical, as opposed to thermal, structure reactivity relationships will be dominated by structure variation effects on DERCOS state structure provides a useful simplification in analysis of the reaction. The DERCOS state, unlike a thermal transition state, is accessible to direct experimental investigation. Luminescent states have long been subject to examination which gives an indication of electronic and vibrational features of the DERCOS state. In recent years, the limitation to luminescent states has been removed. Pulse spectroscopy permits examination of excited state absorption [15], and even population inversion and examination of Raman scattering from excited states [16]. To the extent that appropriate structural information can be extracted from electronic and vibrational spectra of limited resolution, the structure and properties of DERCOS states may be known. No such direct access is available to transition states of interest to the thermal kineticist!

Unfortunately, we do not yet have information on a wide range of DERCOS states. The two best characterized, in the field of transition metal photochemistry, are the charge transfer state of $Ru(bpy)_3^{2+}$ and the ligand field doublet state of $Cr(bpy)_3^{3+}$. Much information has accumulated on properties of the lowest-lying excited state of these two complexes. (By extension some of their relatives with similar ligands are fairly well understood.) The two share one common feature. The ligand is a rigid aromatic system. This fact severely limits the difference between structures of ground and excited states. In the $Ru(bpy)_3^{2+}$ complex, there is a readily measurable difference between potential surfaces of the ground and excited states. In the case of $Cr(bpy)_3^{3+}$, the differences are quite subtle [16]. These two complexes dominate the literature on reactions of long-lived excited states.

(ii) Redox reactions

Photochemical electron transfer was the first type of reaction in which the behaviour of DERCOS states was fully analysed by thermal kinetic techniques. The subject has been extensively reviewed [2]. Only the principles are sketched here.

A DERCOS state may be assigned a standard electrode potential and Marcus–Hush type structure-reactivity correlation may be applied to identify rates of outer sphere electron transfer that should be fast enough to compete with relaxation to the ground state (k_{-1} of eqn. (1)).

Bimolecular outer sphere electron transfer occurs in four steps as follows:

(1) $A \xrightarrow{h\nu} A^*$ excitation

(2) $A^* + B \rightleftharpoons A^*, B$ diffusional encounter

(3) $A^*, B \rightleftharpoons A^+, B^-$ electron transfer

(4) $A^+, B^- \rightleftharpoons A^+ + B^-$ diffusional separation

The reorganization of ligands leading to the transition state occurs in step (3) where the coordination sphere of A^* and B along with the polarization of the surrounding medium adjusts to that appropriate to the activated complex. That this reorganization is required can be seen as a consequence of the Franck–Condon principle. The actual electron transfer may ($K < 1$) and commonly does ($K = 1$) take place after considerable reorganization. In terms of this mechanism, the rate constant for electron transfer is given by:

$$K_{rxn} = K_E \kappa \frac{kT}{h} \exp\left(\frac{\Delta G^\ddagger}{RT}\right) \tag{3}$$

where K_E is the equilibrium constant for step (2), diffusional encounter, and ΔG is the free energy for reorganization of the precursor complex. The other symbols have their common meanings in physical chemistry.

In this case, $\Delta G^{\ddagger}$ can be split into two components. The first is an intrinsic barrier. Reactions where reactants and products have essentially the same free energy (e.g. exchange reactions) have only this intrinsic barrier and its magnitude is estimated from the rate of the exchange reaction. The second is a thermodynamic component of the barrier which can be estimated using the Marcus "cross relation" [17] of eqn. (4).

$$k_{12} = (k_{11} k_{22} K_{12} f_{12})^{1/2} \tag{4}$$

In eqn. (4), k's are rate constants. The subscript 12 refers to a cross reaction, subscripts 11 and 22 refer to exchange reactions. The parameter f_{12} is a function of K_{12}, the equilibrium constant for the cross reaction, k_{11} and k_{22}, and the collision frequency Z. The value of f is near unity in many cases. Some examples of k_{11} and k_{12} values are given in Table 1.

Albery [18] has pointed out that the thermodynamic component will dominate variations of rate with structure for exothermic reaction. Thus, the thermodynamic factor is most important in photochemistry.

The interesting problem for structure reactivity correlation is to estimate K_{12}, the equilibrium constant for reaction of the DERCOS state. This requires values of the electrode potential associated with reactions like those in Table 1, part II. For this purpose the change in the half-cell potential following excitation must be estimated. The thermodynamics of such DERCOS decay channel states have been discussed by Grabowski and Rubaszewska [19].

We consider here the illustrative problem of evaluating the difference

TABLE 1

Rate constants for excited state electron exchange and net reactions

	Reactions	k (M^{-1} s^{-1})	Reference
I.	Exchange (k_{11})		
	$^*Cr(bipy)_3^{3+} + Cr(bipy)_3^{2+}$	10^8-10^9	a, b
	$^*Ru(bipy)_3^{2+} + Ru(bipy)_3^{3+}$	10^8-10^9	a
II.	Net reactions (k_{12})		
	$^*Ru(bipy)_3^{2+} + Cr(bipy)_3^{3+}$	3.3×10^9	c
	$Ru(bipy)_3^{2+} + {}^*Cr(bipy)_3^{3+}$	4×10^8	c

[a] B. Brunschwig and N. Sutin, J. Am. Chem. Soc., 100 (1978) 7568.

[b] N. Serpone, M.A. Jamieson, S. Emmi, P.G. Fuschi, Q.G. Mulazzani and M.Z. Hoffman, J. Am. Chem. Soc., 103 (1981) 1091.

[c] F. Bolletta, M. Maestri, L. Moggi and V. Balzani, J. Chem. Soc., Chem. Commun., (1975) 901.

between the redox potentials for M^+/M and $M^+/{}^*M$ (or M/M^- and ${}^*M/M^-$) couples where M is any metal complex with two oxidation states and the signs + and − only indicate change of charge, not total charge. The first observation is that promotion of an electron from a filled orbital to a higher unfilled orbital simultaneously decreases the ionization potential of the molecule (since the promoted electron may be ionized) and increases the electron affinity (since the hole left by the promoted electron may capture an electron). The remaining factors are summarized in Fig. 2.

In Fig. 2, the potential surfaces with respect to a normal coordinate presumed to relate the reduced form M and oxidized form M^+ are shown. It is assumed here (only as an illustration) that the equilibrium position on the normal coordinate Q is closer to the oxidized form in the excited state ${}^*M$

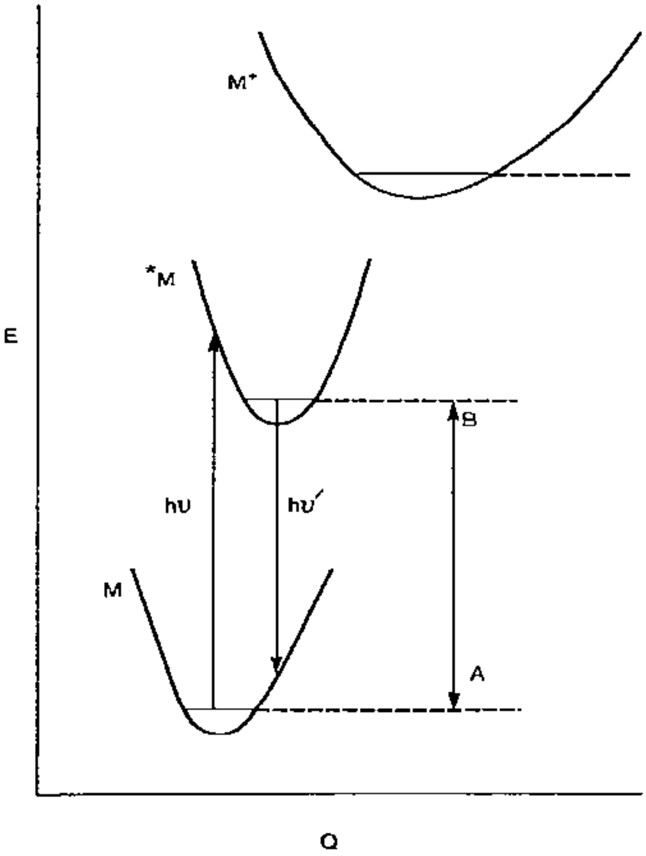

Fig. 2. Potential surfaces with respect to a normal coordinate Q relating the reduced form M, the excited state ${}^*M$ and the oxidised form M^+.

than in the ground state M. Consider reactions with our oxidizing agent $O^{\cdot}$.

$$M + O^{\cdot} \rightleftharpoons M^{+} O^{-} \tag{5}$$

$$^{*}M + O^{\cdot} \rightleftharpoons M^{+} + O^{-} \tag{6}$$

The difference in free energy between the two can be written as:

$$\Delta G(M/M^{+}) - \Delta G(^{*}M/M^{+}) = \Delta H(M/M^{+}) - \Delta H(^{*}M/M^{+}) - T\Delta S(M/M^{+}) + T\Delta S(^{*}M/M^{+}) \tag{7}$$

In eqn. (7), the enthalpy terms may be approximated by ΔE which corresponds to (IP–EA) and is equal to the quantity marked AB in Fig. 2. The entropy term will have three contributions: (a) solvation changes, (b) changes of internal degrees of freedom, and (c) changes in orbital and spin degeneracy. Only the last of these may be calculated with assurance. The ΔE term can be estimated from spectroscopic data. $h\nu$ in Fig. 2 is the energy of the absorption maximum. It is larger than AB. $h\nu'$ is the emission maximum for luminescence and is smaller than AB. If both are available, or vibrational structure is well resolved AB can be satisfactorily estimated.

In practice, successful structure reactivity correlation has so far been limited to metal complexes of bipyridine and 1,10-phenanthroline type ligands. The reason is that these rigid ligands discourage substantial excited state rearrangement. Thus, thermodynamic data are fairly easily derived from spectral parameters. A successful correlation of reactivity with variation of structure has been achieved for charge transfer and ligand field excited states of complexes of ligands in this family with metals Cr(III), Ru(II), Os(II), and Ir(III). Rh(III) has recently been added to the list [20]. The extensive data are thoroughly reviewed by Balzani et al. [2]. The special features of the Cr(III) case are discussed elsewhere in Section C(iii). It is only important to record here that excitation produces large changes in electrode potentials. For example, potentials for $\mathrm{Ru(bpy)_3^{2+}}$ oxidation and reduction move from −1.28 V to +0.84 V and from +1.26 V to −0.86 V. Similarly, potentials for $\mathrm{Cr(bpy)_3^{3+}}$ move from −0.25 V to +1.45 V and from greater than +1.6 v to greater than −0.1 V.

(iii) Examples of DERCOS ligand substitution

We shall begin with a discussion of the solvolytic reaction of $\mathrm{Cr(bpy)_3^{3+}}$. This is perhaps the best documented example of a photosubstitution from a long-lived excited state. The reactive excited state appears to be the ^{2}E which has a lifetime of about 60 μs (although $^{2}T_1$, which is in thermal equilibrium with ^{2}E, may be the immediate precursor of the product).

From the several studies on $\mathrm{Cr(bpy)_3^{3+}}$ [21–23] a general mechanistic pattern has evolved, which is outlined in reactions (8)–(19) for the complex. Excitation of the ground state species, $(^4A_2)\mathrm{Cr(bpy)}_3^{3+}$, into the various quartet manifolds rapidly forms the lowest quartet, $^4T_2$, which might decay

$$(^4A_2)\mathrm{Cr(bpy)}_3^{3+} \xrightarrow{h\nu} (^4T_2)\mathrm{Cr(bpy)}_3^{3+} \quad \text{(excitation)} \tag{8}$$

$$(^4T_2)\mathrm{Cr(bpy)}_3^{3+} \rightarrow (^4A_2)\mathrm{Cr(bpy)}_3^{3+} \quad \text{(non-radiative decay)} \tag{9}$$

$$\rightarrow (^2E,{}^2T_1)\mathrm{Cr(bpy)}_3^{3+} \quad \text{(intersystem crossing)} \tag{10}$$

$$\xrightarrow{\mathrm{H_2O}} \mathrm{Cr(bpy)_3(H_2O)}^{3+} \quad \text{(reactive decay)} \tag{11}$$

$$(^2E,{}^2T_1)\mathrm{Cr(bpy)}_3^{3+} \rightarrow (^4A_2)\mathrm{Cr(bpy)}_3^{3+} \quad \text{(non-radiative decay)} \tag{12}$$

$$\rightarrow (^4A_2)\mathrm{Cr(bpy)}_3^{3+} + h\nu' \quad \text{(radiative decay)} \tag{13}$$

$$\xrightarrow{\mathrm{H_2O}} \mathrm{Cr(bpy)_3(H_2O)}^{3+} \quad \text{(reactive decay)} \tag{14}$$

$$\xrightarrow{\mathrm{OH^-}} \mathrm{Cr(bpy)_3(OH)}^{2+} \quad \text{(reactive decay)} \tag{15}$$

$$\mathrm{Cr(bpy)_3(H_2O)}^{3+} \xrightarrow{-\mathrm{H_2O}} (^4A_2)\mathrm{Cr(byp)}_3^{3+} \tag{16}$$

$$\xrightarrow[-\mathrm{H_2O}]{\mathrm{H^+}} (^4A_2)\mathrm{Cr(bpy)}_3^{3+} \tag{17}$$

$$\xrightarrow{\mathrm{H^+}} \mathrm{Cr(bpy)_2(H_2O)}_2^{3+} + \mathrm{bpyH}^+ \tag{18}$$

$$\mathrm{Cr(bpy)_3(OH)}^{2+} \xrightarrow{\mathrm{OH^-}} \mathrm{Cr(bpy)_2(OH)}_2^{+} + \mathrm{bpy} \tag{19}$$

by non-radiative transitions back to the ground state but instead undergoes intersystem-crossing in about 10 ps [15] with a yield 1.0 [24] to the lowest doublet manifold, ^2E. This initial decay occurs more quickly than the establishment of vibrational equilibrium and cannot be described in a DERCOS state model. It can be predicted as described below from media perturbations in the DOSENCO state limit. This ^2E state is in thermal equilibrium with $^2T_1$. The doublet can react with the solvent to produce what may well be a seven-coordinate intermediate, $\mathrm{Cr(bpy)_3(H_2O)}^{3+}$ (or $\mathrm{Cr(bpy)_3OH}^{2-}$ depending on pH.) The doublet species $(^2E)\mathrm{Cr(bpy)}_3^{3+}$ can also degrade via non-radiative and radiative decay as well.

It is especially interesting that the photochemical "rate law" is found to be identical to the thermal aquation rate law [25] in the pH dependences of the quantum yield for release of bpy into solution, Φ_{bpy}. This identical dependence was taken to mean that the same seven-coordinate intermediate is formed in both instances. Experimental and theoretical arguments indicate that the excited state predominantly responsible for almost all (97%) of the observed photoaquation is a metal-centred doublet. The original arguments are confirmed by a recent wavelength dependence study which shows that decreases in ISC yield at long wavelength correlate to reduction of reaction quantum yield [26]. (More recently, the state responsible was suggested to be the $^2T_1$ which "has a vacant t_{2g} orbital" [22].)

To the extent that the thermally equilibrated, lowest lying, DERCOS doublet manifold (^2E, $^2T_1$) reacts with water ($\Phi_{bpy} = 0.18$, N_2-purged solutions, pH 9–10, $\mu = 1$ M NaCl) to form the seven-coordinate intermediate, the photoaquation must also compete with radiative (reaction (13)) and non-radiative decay of the ^2E state (reaction (12)); the former decay process contributes insignificantly ($\Phi = 10^{-3}$) in the deactivation of $(^2E)Cr(bpy)_3^{3+}$ species but the latter may have an overall yield up to 0.82.

The behaviour of the long-lived $(^2E)Cr(bpy)_3^{3+}$ species towards aquation verifies the suitability of this system as a model of behaviour of DERCOS states. Jamieson et al. [22] have obtained Arrhenius and Eyring activation data from a temperature dependence study of the photoaquation (pH 9.8) of $Cr(bpy)_3^{3+}$; $E_a = 42.6 \pm 1.7$ kJ mol^{-1}, $\Delta H^{\ddagger} = 40.1 \pm 1.7$ kJ mol^{-1}, and $\Delta S^{\ddagger}$ (25°C) $= -41.8 \pm 5.8$ mol^{-1} deg^{-1}. For thermal aquation of $(^4A_2)Cr(bpy)_3^{3+}$ under the same conditions, $E_a = 95.7 \pm 2.5$ kJ mol^{-1}, $\Delta H^{\ddagger} = 93.2 \pm 2.5$ kJ mol^{-1}, and $\Delta S^{\ddagger}$ (25°C) $= -36.8 \pm 7.9$ J mol^{-1} deg^{-1} [25]. A comparison of the kinetic data indicates that the excited state reaction is $\sim 10^{10}$ to 10 times faster, requires considerably less enthalpy for activation, and exhibits about the same entropy lowering in going to the activated complex as does the thermal reaction [22]. Inasmuch as the ^2E and $^4A_2$ states have nearly identical geometry (Stokes' shift ~ 0) [27] the activated complexes from these two states were taken to possess equivalent geometries. The authors originally concluded [22] that: (a) the activated complex arising from ^2E is in an electronically excited state while that from $^4A_2$ is in the ground state; (b) passage of the system from this electronically excited activated complex to the seven-coordinate intermediate proceeds through the excited-state species, $^*[Cr(bpy)_3(H_2O)^{3+}]$, which converts to $Cr(bpy)_3(H_2O)^{3+}$ via a non-radiative process; and (c) that because $^*\Delta H^{\ddagger} < \Delta H^{\ddagger}$, reaction from the doublet manifolds originates with the $^2T_1$ which has been suggested to possess a t_{2g}^3 configuration with one of the orbitals vacant, thus requiring little reorganizational energy to form the electronically-excited activated complex.

These conclusions merit closer analysis for the present purposes. We recognize that very little nuclear rearrangement is associated with the promotion from ^4A to ^2E. This is a well-documented experimental fact, based on extensive absorption and emission measurements under both cryogenic and ambient conditions. Yet, somewhat more than half the enthalpic barrier to substitution has been eliminated and the reaction has been accelerated by 1.5×10^9, neglecting entropy. The mechanism of substitution at d^3 Cr(III) centres generally has been regarded as I_a for some time [28]. The associative barrier has two terms. One is preparation of a bonding orbital for the seventh ligand. The other is nuclear motions to produce seven-coordination. Photon absorption and excitation to ^2E lowers the first barrier considerably but does not lower the second nearly as much. This gives the observationally spectacular rate change from $10^3\,s^{-1}$ to $10^{-7}\,s^{-1}$. (Note that little of the above argument uses ideas unfamiliar to thermal kinetics.)

No other photosubstitution of a demonstrably long-lived excited state has yet been studied in as much depth. This is unfortunate since the $Cr(bpy)_3^{3+}$ example may probably not prove general. The very slight nuclear rearrangement is a special feature of the ^2E state which is a consequence of the fact that both the ground state and the excited state arise from the same configuration, t_{2g}^3 in O_h symmetry. It is, no doubt in part, this fact that causes the excited state reaction to be as slow as it is. The remaining barrier is still 40 kJ mol^{-1}.

Two series of complexes have been studied in sufficient detail to encourage efforts to develop structure-reactivity relationships around the patterns of photosubstitution and photoisomerization. One of these is the series of anionoamine complexes of Cr(III). The problem with these is that ambiguities surround the quantum yields to be associated with the longer-lived, unquestionably DERCOS, doublets. Gutierrez and Adamson [29] have made an interesting attempt to construct a relationship in the case of medium effects on *trans*-$Cr(NH_3)_2(NCS)_4^-$. They begin from the assumption that the main path of doublet relaxation is the reactive pathway (in contrast to radiationless relaxation to $^4A_{2g}$). They then use the lifetimes evaluated from the low quantum yield phosphorescence relaxation pathway as a measure of relative rates of reactive relaxation (i.e. $k_{-1} \ll k_{rxn}$ therefore k_1 can be estimated).

Gutierrez and Adamson [29] examined phosphorescence lifetime in twenty media from water (where a value of 6 ns is found) to the dispersed solid (where the lifetime is 406 ns). Generally, shorter lifetimes are associated with protic solvents such as H_2O, CH_3OH, and even the viscous medium glycerol. Longer lifetimes are found for dipolar aprotic and non-polar solvents: CH_3CN, acetone, sulfolane, and CH_2Cl_2. A common relaxation mechanism was supported by a linear $\Delta H^\ddagger$-$\Delta S^\ddagger$ correlation of the type used by thermal kineticists of the form; $\Delta S^{0\ddagger} = -27.3 - 3.41\ \Delta H^{0\ddagger}$. The short lifetime in protic solvents was attributed to coupling of the complex to solvent vibrational modes. The assignment of reactive decay as determining lifetime is supported by the observation of short lifetime in solvents where thermal reactions are rapid. The apparent activation energies are about half as large as those for thermal substitution.

The limit to this approach is the unresolved question of the range of validity of the assumptions. For example, evidence against a single mode of relaxation emerged from an attempt to test these assumptions by examining solid-state emission as a function of deuteration and temperature [30]. We shall see below that there is evidence for specific decay processes from the quartet in Cr(III) photochemistry that complicates the situation. The theory of Cr(III) reactivity will be considered further after the DOSENCO processes have been introduced. At that point an interpretation opposite to that of Gutierrez and Adamson [29] will be discussed.

The other series of complexes for which a substantial literature exists is comprised by the haloamines of Rh(III) [31]. One of these was chosen as an initial example (Fig. 1) because recent observations of weak solution luminescence by the California group [32,33] support the notion that reaction originates from the lowest-lying ligand field triplet state. This analysis of reaction in conjunction with luminescence lifetime allows explicit assignment of rate constants to the reactive decay path. In the case of $Rh(NH_3)_5Cl^{2+}$, the chloride aquation rate from the excited state is calculated to be 1.4×10^7 s^{-1} (10^{14} times faster than thermal reaction). The rate of NH_3 aquation is 1.5×10^6 s^{-1}. This change of rate corresponds to a reduction of the substitution barrier from the neighborhood of 105 kJ mol^{-1} to something just above 25 kJ mol^{-1}. In the case of the Rh(III) complexes, the reactive excited state is a triplet derived from the electron configuration $t_{2g}^5e_g^1$ (O_h labels) where a σ-antibonding orbital is occupied in the excited state. This should be associated with a substantial nuclear rearrangement on the way to the DERCOS state and changes of nuclear configuration should be prominent in the reduction of the substitution barrier. Observation of solvent sensitivity is in accord with this view [34]. The only clues we presently have as to what these rearrangements are come from the patterns of photoreactivity.

A series of well-defined structure-reactivity relationships has been proposed by Rumfeldt and his students [35–37] at the University of Windsor using their data and earlier reports. These include:

(1) support for Adamson's well-known rule with respect to axis of labilization,

(2) a *trans* effect series for labilization of leaving groups which is $I^- > Br^- > N(CH_3)_3 \sim NH_3 > Cl^-$,

(3) a *cis* ligand effect $NH_3 > N(CH_3)_3 >$ en $>$ cyclam,

(4) an increase in halide yield with pH only for complexes with Bronsted acid amine ligands,

(5) a decrease in amine yields with pH.

An approach to understanding these effects might be made starting from Zink's M.O. analyses [38–40]. this may be premature here, we will return to these points in Section D. Rumfeldt observed that *T* dependence of quantum yields for a wide range of substitution at Rh(III) yields an activation energy about 20 kJ mol^{-1}. Thus, there is clear evidence for limited variation in the step connecting the DERCOS state to the transition state. The important structural variations are to be found in the DERCOS state itself as general considerations above suggested. This can be predicted from Hammond's postulate.

Rumfeldt makes the interesting suggestion that what is here called the DERCOS triplet state corresponds instead to an already dissociated cage-entrapped pair of five-coordinate complex and free ligands. The common 20 kJ activation energy is seen as the barrier of diffusional separation. This suggestion would appear to be ruled out by the observation of luminescence [32,33]. However, the fact that the barrier for reaction is not larger than the barrier for diffusional separation of solvent-caged partners suggests a DERCOS state very similar to the dissociated state. The Rh–X bond (where X represents the leaving ligand) must be quite weak.

(iv) Fundamental features

The major concern of the present section has been examples showing the extent to which photoreaction can be discussed using ideas familiar to the thermal kineticist. The relatively long lifetime of a DERCOS state and its equilibration with respect to vibration allows the key assumption of transition state theory—pseudo equilibration in all degrees of freedom save one—to function as well as it does for thermal reactions. At present, two points merit re-emphasis.

(1) The additional process in reactions of DERCOS states which is not present in thermal reactions is the k_{-1} decay to ground state.

(2) Hammond's postulate suggests common occurrence of a close relation between DERCOS states and transition states for their conversion to product.

If these points are appropriately accommodated, the tools of mechanistic analysis contained in structure-reactivity correlations, and even the mechanistic classifications used in thermal kinetics carry over to photochemistry. This will not be true of the DOSENCO processes we discuss next. Consequently, a new model will be considered.

C. STATES DECAYING ON A SPECIFIC NUCLEAR COORDINATE (DOSENCO)

(i) General considerations

Absorption of visible or near UV photons promotes metal complexes directly to states with energies well above both experimental and theoretical estimates of the barriers for dissociative substitution or isomerization. Similarly, these energies are above barriers for most common electron transfers. Thus, it is not at all unexpected that crossover to dissociative states can

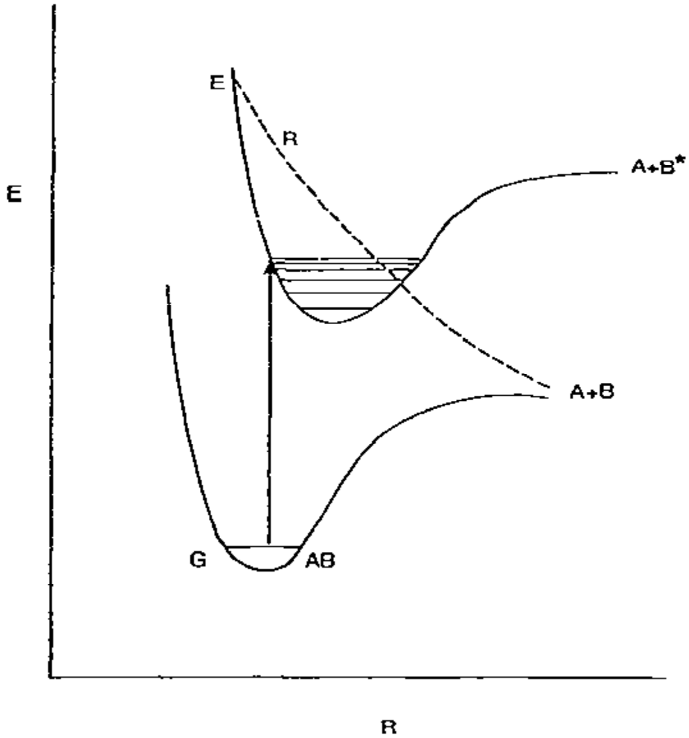

Fig. 3. Description of predissociation in diatomic molecules.

occur. Predissociation is a well-known process in diatomic molecules. A description of how it arises is given in Fig. 3. It has similarly been documented in a number of cases for small polyatomic molecules [41]. Moreover, dissociation above the convergence limit is very rapid. As an example consider the photodissociation:

$$Cl_2CS \xrightarrow{h\nu} ClCS + Cl \qquad (20)$$

Pressure dependence (quenching) studies [42] show that the lifetime of the excited state ($^1A_2$) is 55 ns on 4358 Å excitation, 6 ns on 3660 Å excitation and "unmeasurably" short on 2537 Å excitation. These results can be related to the observation that fluorescence is observed with excitation longer than 4500 Å. The absorption shows fine structure in the region 4000–6000 Å but the absorption spectrum shows no structure near 2357 Å.

In condensed phases, spectra of large molecules like metal complexes are not generally well resolved and it is difficult to identify processes analogous to predissociation from examination of absorption spectra. The matter is extremely complex because of the large number of degrees of freedom involved. Pictures like Fig. 3 can only be suggestive, not descriptive. The most common indication of states which decay on a specific nuclear coordinate (DOSENCO) is the wavelength dependence of quantum yield over a wavelength range where the competing processes are a well-characterized reaction versus some identified vibrational relaxation process.

In describing wavelength dependence in solutions, the simplest physical model is that introduced by Franck and Rabinowitsch [43] which calls attention to the role of kinetic energy of a separating fragment. At shorter wavelength, the higher energy of the dissociating fragment increases the probability that it will escape the solvent cage and consequently reduces the probability of geminate recombination (or back reaction of any sort) limiting the observed quantum yield. This is certainly one way in which the initial excitation energy can influence quantum yield but of course, this requires retention of the initial kinetic energy in competition with collisional deactivation by solvent. It can only be significant on very fast time scales. In transition metal complexes, for example, this mechanism is suggested to account for the wavelength dependence of oxygen yields from MnO_4^- [44,45]. Since this ion does not fluoresce even in low T solid matrices, there is independent evidence that the excited state lifetime is less than 5 ns.

The cage escape model does not exhaust the possibilities. Considering diatomic states E and R in Fig. 3 again, we can recognize that crossing from states E to R in competition with vibrational relaxation to the 0th vibrational states of E can depend on the excitation wavelength and the initial degree of vibrational excitation. Moreover, it is not improbable that a large molecule in a condensed phase can dissipate excitation to the surroundings quite rapidly. Thus, wavelength dependence may not be a consequence of the Franck–Rabinowitsch cage effect at all. It is quite possible that a geminate pair produced from a dissociative state will be thermalized prior to separation. The wavelength dependence will then have to do with the "relaxability" of the initially populated vibronic (or better rovibronic) state. That is, our attention must focus on specific dynamic processes of molecules at high levels of excitation.

There are two fundamental theoretical strategies open for the investigation of the problem of the dynamic processes that determine DOSENCO state reactivity. One is pursuit of the solution to the relevant differential equation. The other begins from a recognition that every differential equation has a group [46]. From this point of view an effort can be made to isolate the constants of motion of allowed processes (perturbation theory often tends to lose sight of such fundamental physics) and explore the possibility of developing relevant selection rules. The final section of this paper reviews approaches to the problem of DOSENCO state mechanisms from the group theoretic point of view. However, we must review first some experimental evidence relevant to well-studied systems which may exhibit DOSENCO state photoprocesses. We try to show that at least enough experimental cases are now established to motivate the theory.

(ii) Metal carbonyl complexes

A well-known system recently reviewed in detail elsewhere [47] provides an instructive first example which may represent the simplest case to characterize in the DOSENCO state limit. This is the wavelength dependence associated with photosubstitution in $M(CO)_5L$ where $M = Cr$, Mo, or W; and L is a ligand typified by pyridine.

At the outset, it is useful to observe that substitution into $M(CO)_6$ proceeds dissociatively to give an intermediate, $M(CO)_5$ which has been characterized spectroscopically in low-temperature glasses [47]. Excited states of $M(CO)_6$ have not been found to fluoresce at any T, but luminescence of $Cr(CO)_6$ can be sensitized by toluene at low T [48]. This indicates subnanosecond lifetime. Consequently, the dissociation must be quite fast. It is reasonable to assume a similar behaviour for $M(CO)_5L$ in reactions shown in eqns. (21) and (22).

$$M(CO)_5L \xrightarrow{h\nu} M(CO)_4L + CO \tag{21}$$

$$M(CO)_5L \xrightarrow{h\nu} M(CO)_5 + L \tag{22}$$

In these two competing reactions, wavelength dependence is observed [49,50]. The quantum yield for CO loss decreases at longer wavelengths. Loss of L, however, becomes more important at longer wavelengths.

One possibility is that loss of CO becomes more important as the initial degree of vibrational excitation is increased but there is an alternative explanation that requires a less stringent limitation on the extent of vibrational relaxation preceding the crucial events leading to dissociation. The C_{4v} symmetry species $M(CO)_5L$ has two ligand field states, one of which corresponds in the strong field limit to population of the in-plane d^*_{xy} orbital and the other which corresponds to population of the $d^*_{z^2}$ axial orbital. Since CO is the stronger field ligand, the first of these states is higher. One can now explain the wavelength dependence of reactions (21) and (22) by assigning (21) to the state with d^*_{xy} population and (22) to the state with $d^*_{z^2}$ population. (This idea is supported by the stereochemistry of incorporation of ^{13}CO into two $Mo(CO)_5$ piperidine complexes [51].) In this view, loss of CO from the upper state is competitive with internal conversion to the other ligand field state! Since overall excited-state lifetimes are short, this internal conversion must be (as it would be expected to be) a quite rapid radiationless transition. Yet, the CO loss rate is competitive. It is clear that the same theoretical approach used to describe the fast internal conversion must be used to analyse the rate constant for CO loss. After the consequences of these observations have been appreciated, it is easier to accept the alternate idea that the degree of initial vibrational excitation is important. We need a full analysis of the dynamical processes connecting states of the system.

(iii) Cr(III) amine complexes

In the earlier literature on the photosubstitution reactions of Cr(III) complexes, some more or less definite lines of evidence pointed to reaction for the ^2E state (O_h symmetry) on the one hand and from the ^4T state on the other. Emergence of definite evidence for the substitutional reactivity of the quartet was the beginning of the development of evidence for prompt reactions that require DOSENCO theory. Studies exploiting luminescence were very important.

In 1970, Chen and Porter [52] demonstrated by quenching of the "^2E" of $Cr(NH_3)_2(NCS)_4^-$ in a fluid at −65°C with $Cr(CN)_6^{3-}$ that 50% of the SCN^- solvolysis yield arose from the quartet prior to intersystem crossing. Following Kane-Maguire and Langford's observation [53] that doublet phosphorescence was observable in many fluids and exhibited T dependence consistent with lifetimes limited by back intersystem crossing to the quartet, several room temperature examples of the Chen and Porter phenomenon were recorded. For example, incomplete quenching of substitution reaction in $Cr(NH_3)_6^{3+}$ [54] and $Cr(en)_3^{3+}$ [55] and incomplete quenching of isomerization of $Cr(phen)_3^{3+}$ [56] were observed. Similarly, substitution in $Cr(CN)_6^{3-}$ could not be sensitized with doublet sensitizers [57]. It occurs only on direct quartet excitation.

Such results converge to establish that there exist pathways for quartet reaction determined prior to intersystem crossing to the doublet. An indication of the timescale first emerged from the observation by Kane-Maguire et al. [58] that the intersystem crossing yield for $Cr(en)_3^{3+}$ is wavelength dependent across the envelope of the first quartet band. This established that intersystem crossing competes with vibrational relaxation. Shortly thereafter Kirk et al. [15] reported picosecond pulse experiments indicating intersystem crossing in a few picoseconds. Subsequent work has confirmed picosecond lifetimes for Cr(III) quartets by doublet-excited state absorption grow-in measurements [59,60] and quartet saturation experiments [16]. Thus, events determining entry to a reactive pathway occur on the picosecond timescale in competition with vibrational relaxation. This would appear to put photosubstitution originating from the quartet firmly in the DOSENCO state limit. The alternative notion that the fast process is a partitioning of paths to a long-lived DERCOS quartet and the doublet does not appear to be consistent with recent spectroscopic probes of the quartet itself [16,60].

Given that reactions in the quartet can be rapid, it is interesting to explore evidence from wavelength dependence within the envelope of one absorption band. Most such studies depend for precision on measuring the relative yields for two competing reactions. Wavelength dependence is not observed in all such cases. For example, *trans*-$Cr(en)_2(NCS)_2$ shows constant yields for solvolytic loss of both NCS^- and one end of the en chelate ring from 400 — 580 nm. Both of these are identified as reactions from the quartet by quenching experiments and observations of wavelength dependence of the intersystem crossing yield [61]. However, a considerable series of careful studies (especially including those by Kirk et al. [15]) demonstrate small but definite wavelength dependence in the ratio of competing paths. Some examples follow. The Bologna group reported wavelength dependence in the en ring opening of *trans*-$Cr(en)_2(NCS)Cl^+$ whereas Cl^- or SCN^- loss yields were wavelength independent [62]. The complex is C_{4v} where ^4T splits to $^4B_2$ and ^4E. The constant anion loss yields were attributed to ^4E while the wavelength dependent reaction was attributed to the higher $^4B_2$ state. Wong and Kirk [63] report more or less exclusive NH_3 loss from *trans*-$Cr(en)_2(NH_3)Cl^{2+}$ on excitation into ^4E at 546 nm but reduction of the yield for this path was accompanied by some en ring opening at 436 nm ($^4B_2$). Rosebush and Kirk [64] report a similar increase in en ring opening (versus Br^- photosolvolysis) at shorter wavelength in a study of *trans*-$Cr(en)_2Br_2^+$. Finally, examples of similar behaviour are also found with *trans*-$Cr(en)_2Br_2^+$ [65]. Very recently [66] Kirk, Frederick, and Glover have established that SCN^- photoaquation of *trans*-$Cr(en)_2(SCN)\ F^+$ is quenched in parallel with emission while en photoaquation is quenched to a lesser extent. These results are inconsistent with suggestions that have attributed different modes of reaction to the two-spin states (quartet and doublet). The wrong mode is quenched in parallel with emission.

All these wavelength dependence results require at least a comment similar to that made about $M(CO)_5L$ complexes. The distinguishable reactivity of two neighboring ligand field states requires reaction pathways to be selected in competition with internal conversion of closely spaced states. However, we can now add that we know that overall quartet state lifetimes in closely related molecules are picosecond. These facts recommend a DOSENCO state analysis in the language of this review. This view is emphasized by one additional recent study. The photoracemization of (−)-$Cr(phen)_3^{3+}$ was shown to display a non-quenchable quartet component which could be attributed to reaction preceding intersystem crossing [56]. This non-quenchable quartet component shows wavelength dependence that was attributed to initial excitation of progressively higher vibronic levels. The authors' conception was of an isomerizational analog of a dissociation limit [41].

(iv) Co(III) amine photochemistry

The Co(III) amines are a convenient series for examination of the subtle effects of structure variation because of the ease of synthesis of a large family of closely related complexes. However, they have proved a bit of a disappointment to photochemists: quantum yields for ligand substitution are low [67]. Characteristic ligand substitution quantum yields under irradiation of ligand field (L.F.) bands are only $10^{-3}-10^{-4}$. The L.F. photochemistry is now well characterized. The use of CW laser techniques on samples in small volume cells as introduced by Adamson's group [68,69] has yielded suitably precise results. The first point to be made is that the photolysis rules developed by Adamson for Cr(III) amines are relevant to Co(III) photosubstitution as well. However, wavelength dependence is much more pronounced than it is in Cr(III) cases. In order to understand this wavelength dependence, it is necessary to comment on the photoreduction which follows ligand to metal charge transfer (LMCT) excitation.

Endicott et al. [70] pointed out that the E_{max} of a ligand to metal charge transfer band may be estimated as a sum of enthalpy terms for electron transfer within an ion-pair complex according to eqn. (23).

$$E_{max}(\text{LMCT}) = \Delta H^0_{IP} + \Delta H^{\ddagger} + \frac{\lambda}{4} - E_B \tag{23}$$

In (23), ΔH^0_{IP} represents the enthalpy of formation of an ion-pair complex, $\Delta H^{\ddagger}$ is the activation enthalpy for fission of the metal–ligand bond as determined from the temperature coefficient of the thermal substitution reaction, λ is a ligand rearrangement energy from Marcus theory, and E_B is a bond energy for the interaction of radicals. The threshold of LMCT absorption should occur at ($E_{max} - \lambda/4$). Since the onset of photoredox chemistry begins very near the threshold, there is little barrier to such reaction. However, wavelength dependence of redox photochemistry shows that some "Franck–Condon" reorganization is involved but reaction occurs in competition with solvent relaxation (probably 100 ps time scale). It may be noted that recent picosecond pulse experiments by Endicott and Netzel [71] demonstrate homolysis of a Co–alkyl bond in less than 8 ps.

These considerations allow construction of an energy diagram for the overall photochemistry of a Co(III) complex including photosubstitution. The interesting case of $Co(NH_3)_5N_3^{2+}$ [72] which photoaquates to release both NH_3 and N_3^- in measurable quantities is so diagrammed in Fig. 4. In this figure, $\Delta H_1^{\ddagger}$ and $\Delta H_2^{\ddagger}$ represent the activation enthalpies for thermal loss of N_3^- and NH_3 respectively (ΔH_c^0 is the enthalpy for formation of a $Co(II) \cdot N_3$ radical pair).

The presently important point of the figure is that several of the DERCOS

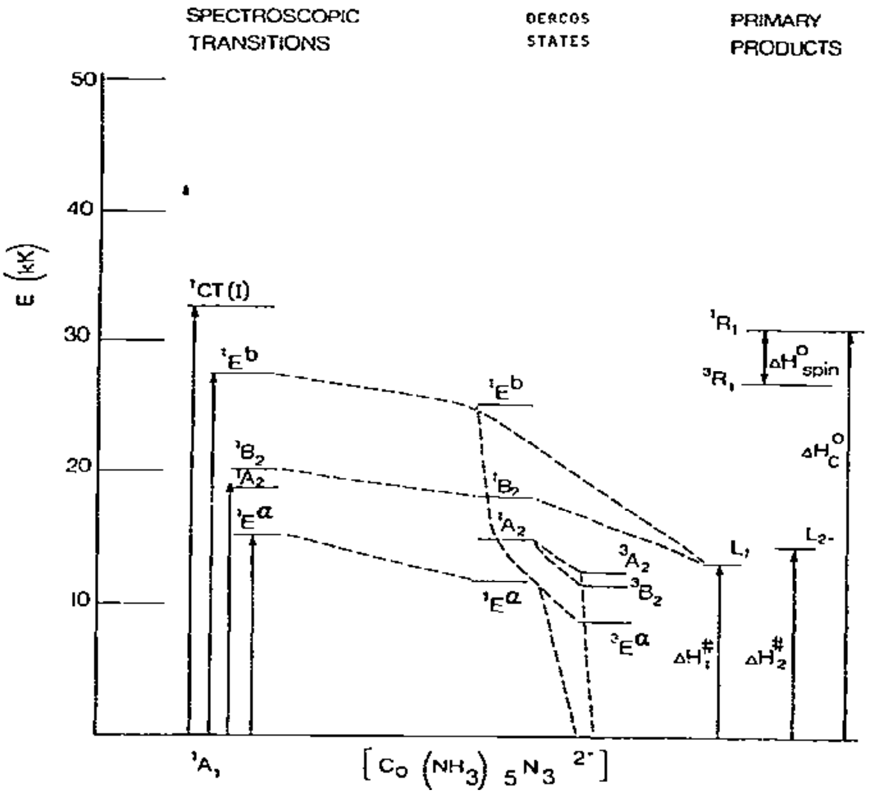

Fig. 4. An energy state diagram for the photochemistry of a Co(III) complex.

states lie *below* the transition states for thermal substitution. The figure suggests substitution occurs via relaxation through these transition states (i.e. a hot ground-state reaction). Whether this is precisely correct or not, it is clear that unless the thermal reactions are aided by quite abnormal values of frequency factors, the photochemical substitution cannot occur via a state of lower energy than the thermal transition state. This is because transition state theory assures us that the thermal reaction occurs through randomly selected channels, selected only as an inverse function of the different energy barriers. The saddle point is crossed.

The consequence is that substitution reaction always occurs on a pathway of relaxation which competes with relaxation to the lowest DERCOS state of either spin manifold. Any molecule reaching the lowest DERCOS state is unreactive according to this analysis because the energy is too low. The small quantum yields for substitution are understandable. Internal conversion is efficient and only a fraction of molecules is diverted to the reactive path which must occur directly from a DOSENCO state. The wavelength dependence systematically observed becomes an indication that entry to the reactive path can depend on the initially excited vibrational modes.

It is quite interesting that extension of studies of $Co(NH_3)_5Cl^{2+}$ to irradiation of the "triplet" region using a 647.1 nm Kr-ion laser line showed that NH_3 aquation which occurred in preference to Cl^- aquation at 514 nm was greatly diminished but that the yield for Cl^- aquation was only slightly diminished [73]. This result is entirely in agreement with the interpretation given in Fig. 4.

As was noted above, to a first approximation, yields for photosubstitution follow the same pattern as a function of structure as do the much larger substitution yields for Cr(III) (Adamson's rules). However, photosubstitution stereochemistry is not quite like that for Cr(III) [74]. Of course, adherence to Adamson's rules is found in experiments using 488 or 514 nm irradiation. The rules fail at 647.1 nm where reversal of ligand loss preference is observed. This change only gives emphasis to the specific character of events leading to substitution.

D. THEORY OF DECAY OF PHOTOEXCITED STATES

(i) Mechanistic interpretation of the Golden Rule

At several places above, we have made passing reference to theory, but explicit consideration has been deferred in order to first clarify the issues that theory must confront. In particular, since the tools of thermal kinetics cannot be used for DOSENCO processes, a model for such processes is much needed.

The very interesting molecular orbital discussions exemplified by Zink [38] have not distinguished between DOSENCO processes at the rapid limit, and the DERCOS state slow limit. This is because Zink used ligand field parameters validated from band maxima of absorption spectroscopy. Parameters from absorption band maxima are parameters of "vertical" transitions and retain ground-state geometry.

Zink has been criticized for his inability to account for competition between rates of reaction, radiationless return to the ground state, and luminescence. The critics have failed to appreciate that his notable success may follow from the fact that his work does implicitly contain a partial account of this competition. The "vertical" ligand field parameters give an indication of the likely nature of rapid DOSENCO processes in the sense of a "theory of relaxability" introduced by Devaquet [75], which suggests that parameters from vertical transitions and ground-state geometry could be used to identify the most favourable "initial" directions of relaxation of an excited state. This indication of initial direction may be useful in both the DERCOS and DOSENCO state limits, but is most valuable in the DOSENCO state case. However, in the slow reaction limit, it indicates the direction (in the sense of nuclear motions) toward the DERCOS state. As was argued above, the DERCOS state is likely to be similar to the transition state for photoreaction so that information on the DERCOS state does give indication of reactivity. Basically, Zink's approach tackled the behaviour of DOSENCO states. This is the area in greatest need of theory since mechanistic tools of thermal kineticists cannot be applied. Zink's theories are limited by omission of explicit consideration of vibronic coupling. (This is recognized by Zink's recent interest in analysing excited state parameters via Franck–Condon analysis of luminescence spectra [76].)

Beyond the theories of bonding in the excited state, there has been an effort by Vanquickenborne and Ceulemans started in 1977 [80,81] to develop correlational selection rules. The spirit of the work is very close to the Woodward and Hoffman [77] orbital correlations and the (more rigorous) Longuet-Higgins and Abrahamson [78] state correlation. The theory has recently been used to account for the subtle and challenging pattern of the stereochemistry of photosubstitution at Cr(III) [10]. Kirk who first pointed out the full implications of stereochemistry for testing mechanistic ideas, judged the Vanquickenborne–Ceulemans theory quite successful [79]. Figure 5 shows a scheme based on the assumption that a photosubstitution on $Cr(NH_3)_5F^{2+}$ begins dissociatively, involves two states (^4E and $^4B_2$ in C_{4v}), and undergoes rearrangement according to the selection rules, to prepare the system for entry of a solvent ligand. It may be observed that the treatment based on dissociation is simple and clean but does not exclude the associative path that would be more complex to represent. In fact, Zink [80] has carried out some correlation calculations with the higher coordination numbers for metal centres required by an associative path.

Vanquickenborne and Ceulemans' approach introduces an idea we wish to pursue—development of selection rules. The problem that a theory of behaviour of DOSENCO states must address is the explicit description of transitions between states. Some initial approximate wave function can be given for the state achieved by absorption of a photon. However, in order that the spectroscopic state can be assigned readily, the Hamiltonian is usually simplified in a way that reveals strong selection rules in the event of photon absorption. The states subject to the strong selection rules are the "zero-order states" referred to in most of the experimental discussion above. This means that the total Hamiltonian is, $H = H_M + H_F + H_{int}$, where H_M is

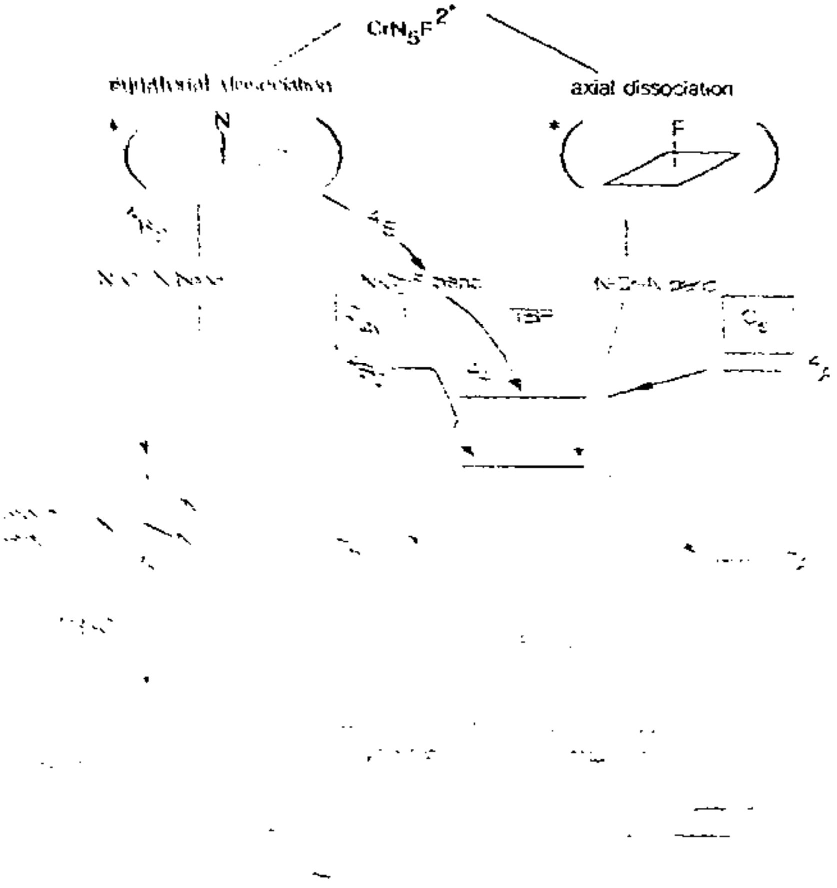

Fig. [illegible] Correlation diagram [illegible] in CrN_5F

the molecular Hamiltonian, H_R is the Hamiltonian of the radiation field, and H_{int} is the interaction induced by the field. It is usually then written as a sum of a zero-order Hamiltonian H^0 and a perturbation H' as follows:

$$H = H^0 + H'$$

where

$$H^0 = H_M + H_R \text{ and } H' = [illegible]$$

It is the term which [illegible] used to assign the absorption spectrum. [illegible] with coupling the zero-order molecular states to provide the time evolution [illegible] states that is called "radiationless transition" [illegible]. When energy is simultaneously [illegible] ferred to the environment, especially via vibrational and rotational energy interactions, the process becomes the characteristic irreversible radiationless transition. Of course DOSENCO photochemistry is just a class of radiationless transitions.

The rate of this radiationless process has been expressed as a product of coupling and density terms called the "Golden Rule" [81].

$$k(\mathrm{s}^{-1}) = \frac{2\pi}{h}|V_{mn}|^2\rho_m \tag{25}$$

where $|V_{mn}|^2$ is the probability associated with the matrix element, $\langle m|V|n\rangle$, which couples the initial zero-order state $|n\rangle$, and a final state $|m\rangle$. Here $|m\rangle$ is an electronic state with a high density of vibrational components nearly isoenergetic with $|n\rangle$, and ρ_m is the density of states in the closely packed set of coupled states $|\{m\}\rangle$. The golden rule is useful where the set $\{m\}$ approximates a classical continuum. This model can provide a statistical description of rates but obscures the selection rules inherent to the process.

In organic mechanistic photochemistry an alternative expression has been developed which allows for clarification of the quantum mechanical selection rules. Instead of identifying a probability based on a single coupling mechanism and the density of all other states, the rate can be written as a fundamental rate multiplied explicitly by all of the couplings which arise from each of the important physical interactions [81];

$$r_{\mathrm{obs}} = r_{\mathrm{fund}} \cdot \sum_{e,v,s} f_e \cdot f_v \cdot f_s \tag{26}$$

The inhibition factors f_i are numbers equal to or less than unity which can be derived from the matrix elements of electronic, vibrational, or spin coupling. In current models this scalar factorization relies on the Born–Oppenheimer approximation [82].

Our objective here will be to give a precise quantum mechanical foundation for the partitioning expressed by eqn. (26) independent of the Born–Oppenheimer approximation. The result will provide guidance to identification of selection rules influencing f_e, f_v, and f_s without requiring the limitations of the Born–Oppenheimer approximation.

At the beginning, some remarks on the value of r_{fund} are useful. For a spin-conserving unimolecular radiationless transition involving limited change of nuclear coordinates, this rate is of the order of $10^{13} - 10^{14}\ \mathrm{s}^{-1}$ and is limited by the time it takes nuclei to execute zero point motions [82]. When we consider photoprocesses of transition metal complexes we must consider the metal–ligand vibrations of lower frequency. An energy of 500 cm^{-1} and a process of ligand exchange, which will require large excursions along a vibrational coordinate, may bring r_{fund} down to values below 10^{12} s^{-1}.

Regardless of the form of the rate equation, in the conventional approach to evaluating these coupling factors, one makes a series of simplifying assumptions based on reasonable but classical, physical analogies of the possible decay routes. The major contributing mechanism to decay of electronically-excited states is assumed to be vibronic coupling to available normal modes of the molecule. The model is further simplified using the Born–Oppenheimer approximation which requires weak coupling between bases. This permits the use of adiabatic basis functions in calculating the inhibition factors. There are many indications however, that this is an oversimplification in the case of allowed decay processes where strongly coupled diabatic functions are needed [11]. The chief importance of the Born–Oppenheimer approximation is that it allows the electronic and vibrational factors to be written as a simple scalar product of separate matrix elements. In most systems the electronic matrix element can be evaluated by one of many available techniques. The vibrational element is usually factored further, using the Franck–Condon principle [82], into a scalar product of a promotion mode matrix element and a Franck–Condon normal mode overlap factor. Considerable effort has been spent on evaluation of these latter factors but by classical analogy they are largest when the nuclei are moving very slowly. Thus, particularly for high vibrational overtones of the excited states, transitions between states in this model tend to occur near the turning points of normal modes.

This Born–Oppenheimer/Franck–Condon model has been useful in constructing a semiquantitative understanding of decay processes. However, its predictive power has been limited to numerical calculation of relative decay probabilities, in cases such as isotopic substitution or heavy atom substitution, and some very general conclusions concerning the ergodicity of the redistribution of excitation energy into highly-degenerate normal modes [83]. The greatest difficulty with this formalism is the absence of simple but comprehensive selection rules which can transcend the approximations and the appeals to classical analogies.

(ii) Tensorial selection rules for transient events

These selection rules can be derived through an alternative approach to the problem. Instead of placing emphasis on the nature and extent of various plausible coupling mechanisms we will focus initially on obtaining an adequate description of the transient event itself. This event, which is observable directly or indirectly, can be factored into physically reasonable contributions later, after the phenomenon itself has been completely characterized. In a group theoretic sense, we will consider a description of the observable event to be complete when the basis vectors, representing both the observable states and the transition moment operators, are given enough quantum mechanical characteristics to establish all required orthonormality conditions. In mathematical terms, the matrix for the operator is then diagonal. This requirement very often means that representation and component labels derived from the finite-point group of the molecule are insufficient to fully characterize states and operators. The problem is encountered routinely in ligand field theory [84] and is resolved [85] by appeal to generative groups of higher symmetry which may include infinite groups requiring more than three dimensions. In practice this inductive appeal to higher groups is reversed to become a subduction technique in which the molecular operators and states are projected out of the sufficiently large generative group by a unique hypergeometric algebra [86]. In this connection, the physical meaning of the appeal to higher groups becomes clear. Within the generative group in which no coupled interactions are present, both the kinetic and potential terms in the Hamiltonian are fully symmetric. The subduction to lower symmetries involves the addition of new potential terms which may be of lower symmetry, but the selection rules associated with the behaviour of the totally symmetric kinetic energy operator in the generative group are not lost. As a result, selection rules for finite group matrix elements can be factored with physical significance into scalar products of selection rules in all the necessary higher groups [85]. If any one of these selection rules vanishes the entire matrix element must vanish in the particular order of approximation employed.

While such procedures are well established in the calculation of ligand field energy levels they are not formally limited to this particular group of compounds, or to calculations involving only this Hamiltonian. The same formalism can be generalized to describe operators and states of any quantum mechanical system or event and will form the basis for our investigation of selection rules intrinsic to, and highlighted by the inhibition factor form of the golden rule. The phenomenological form of the golden rule, that is the expression of the rate of the observable process before any theoretical factorization is imposed, can be stated as

$$\begin{aligned} r_{\mathrm{obs}} &= r_{\mathrm{fund}} \Sigma \int_{T,\Gamma,\gamma} \Psi^{\gamma'}_{T'\Gamma'} \mathrm{D}^{\hat{\gamma}}_{\hat{T}\hat{\Gamma}} \Psi^{\Gamma}_{T\Gamma} \, \mathrm{d}\tau . \\ &= r_{\mathrm{fund}} \sum_{T,\Gamma,\gamma} C \langle T' \Gamma'_T \gamma'_T | \hat{T} \hat{\Gamma}_T \hat{\gamma}_T | T \Gamma_T \gamma_T \rangle \end{aligned} \tag{27}$$

The two versions of the rule are related by a unitary transformation from the matrix element evaluated by integration in displacement space, to the Dirac tensorial bracket evaluated using the Wigner–Eckart theorem algebra in magnetic moment vector space. Here T, Γ, and γ are the infinite group representation, the finite-group representation, and the finite-group component labels for basis functions respectively. The matrix element integral form requires a solution of the differential equation for the moment operator and often involves numerical methods which obscure the selection rules based on the constants of motion. The Dirac bracket form, in contrast, permits a straightforward calculation of the selection rule conditions by tensor algebra techniques and is readily adapted to describing coupled systems. The bracket is evaluated by applying the Wigner–Eckart theorem which assumes complete separation of angular and radial terms

$$\begin{aligned}\langle T'\Gamma'_T\gamma'_T|\hat{T}\hat{\Gamma}_T\hat{\gamma}_T|T\Gamma_T\gamma_T\rangle = \quad & \underset{\text{(a)}}{(-1)^{J(\Gamma'_T)+\gamma'_T}}\underset{\text{(b)}}{\begin{pmatrix} T' & \hat{T} & T \\ \Gamma'_T & \hat{\Gamma}_T & \Gamma_T \end{pmatrix}} \\ & \times\underset{\text{(c)}}{\begin{pmatrix} \Gamma'_T & \hat{\Gamma}_T & \Gamma_T \\ \gamma'_T & \hat{\gamma}_T & \gamma_T \end{pmatrix}}\underset{\text{(d)}}{\langle T'||\hat{T}||T\rangle}\end{aligned} \tag{28}$$

This factorization yields the product of a phase factor (a) with a partition coefficient (b), a 3Γ symbol [87] describing permitted couplings of a vector component (c), and a radial reduced matrix element (d). The phase factor depends on the numerical assignment $J(\Gamma'_T)$ of the molecular group representation Γ'_T and on the numerical value of the component γ'_T. The partition coefficient [85] describes the linear combinations of the bases labelled by T's in the generative group after subduction onto the bases labelled by Γ's in the molecular group. The 3Γ symbol expresses the representation and component selection rules of the finite molecular group and is evaluated for non-vanishing cases from orthonormality conditions. Finally, the reduced matrix element is a scalar quantity expressing, in the case we are concerned with, the size of multipole moment effects referred to the generative group.

Without pursuing these evaluation procedures in further detail, it is clear that the bracket describing the decay event provides selection rules in the molecular group through the 3Γ symbol and in the generative group through the partition coefficient. If either term vanishes, the event is forbidden in the chosen order of approximation. Both types of symbol have been tabulated for point groups of interest in inorganic chemistry [85,87] but there is no formal reason for restriction of their use to this area alone. Indeed recent work has shown that they are equally useful in assigning the spectra of aromatic hydrocarbons and their heteroatom derivatives [88].

Having achieved our initial objective of deriving a complete description of observable quantum events, we can now return to the question of factoring such events into changes in coupled physical processes. This factorization is done to provide some physical insight into the overall event, usually on the basis that the phenomena are weakly coupled. However, this traditional Born–Oppenheimer approximation is unnecessary, both for the purposes of mathematical simplicity and physical understanding. Indeed the rapid, highly probable events of interest in photochemistry usually occur under strong coupling conditions of spin, orbital, or vibrational vectors. Using the complete basis vectors and operators just described, the strength of the coupling is irrelevant to the desired factorization. The formalism of uncoupling is identical to that used in intermediate ligand field theory [85] and in both cases, the magnitude of the coupling has no effect on the method of the factorization calculation. Using vibronic coupling initially, the complete basis sets can be restated as uncoupled scalar products of electronic and vibrational basis sets,

$$|T\Gamma_T\gamma_T\rangle = \sum_{\substack{J,V\\ \Gamma_J,\gamma_V\\ \Gamma_J,\gamma_V}} (-1)^{J(\Gamma_J)+J(\Gamma_V)+\gamma_T^*} \frac{(2T+1)^{1/2}}{\lambda[\Gamma_T]} \begin{pmatrix} \Gamma_J & \Gamma_V & \Gamma_T \\ \gamma_J & \gamma_V & \gamma_T^* \end{pmatrix} \times \begin{pmatrix} J & V & T \\ \Gamma_J & \Gamma_V & \Gamma_T \end{pmatrix} |J\Gamma_J\gamma_J\rangle\ |V\Gamma_V\gamma_V\rangle \qquad (29)$$

The uncoupling procedure involves a summation of the product functions over all contributing electronic and vibrational states at both the finite and infinite group levels. In general therefore, the single observable event is described by well-defined sum of allowed combinations of electronic states with specific normal modes. In order to predict which of these combinations are allowed we must first investigate the behaviour of the transition moment operator for both the electronic and vibrational systems separately. The behaviour of the total moment $|\hat{T}\hat{\Gamma}_T\hat{\gamma}_T|$ will then be determined by which factored moment obeys the more limiting selection rules.

To first order, these overall selection rules will be defined in terms of the electronic and vibrational selection rules derived from the uncoupling procedure. The uncoupled operator has the form;

$$|\hat{T}\hat{\Gamma}_T\hat{\gamma}_T| = \sum_{\substack{\hat{J},\hat{V}\\ \hat{\Gamma}_J,\hat{\Gamma}_V\\ \hat{\gamma}_J,\hat{\gamma}_V}} (-1)^{J(\hat{\Gamma}_J)+J(\hat{\Gamma}_V)+\hat{\gamma}_T^*} \frac{(2\hat{T}+1)^{1/2}}{\lambda[\hat{\Gamma}_T]} \times \begin{pmatrix} \hat{J} & \hat{V} & \hat{T} \\ \hat{\Gamma}_J & \hat{\Gamma}_V & \hat{\Gamma}_T \end{pmatrix} \begin{pmatrix} \hat{\Gamma}_J & \hat{\Gamma}_V & \hat{\Gamma}_T \\ \hat{\gamma}_J & \hat{\gamma}_V & \hat{\gamma}_T^* \end{pmatrix} |\hat{J}\hat{\Gamma}_J\hat{\gamma}_J V\hat{\Gamma}_V\hat{\gamma}_V| \qquad (30)$$

Then, by combining eqns. (28), (29) and (30)

$$
\begin{aligned}
\langle T'\Gamma'_T\gamma'_T|\hat{T}\hat{\Gamma}_T\hat{\gamma}_T|T\Gamma_T\gamma_T\rangle = & \sum_{\substack{J',\hat{J},J\\ \Gamma'_J,\hat{\Gamma}_J,\Gamma_J\\ \gamma'_J,\hat{\gamma}_J,\gamma_J}} (-1)^{J(\Gamma'_J)+J(\Gamma'_V)+\gamma'^{*}_T}\\
& \times(-1)^{J(\hat{\Gamma}_J)+J(\hat{\Gamma}_V)+\hat{\gamma}^{*}_T}\cdot(-1)^{J(\Gamma_J)+J(\Gamma_V)+\gamma^{*}_T}\\
& \times\frac{(2T'+1)^{1/2}(2\hat{T}+1)^{1/2}(2T+1)^{1/2}}{\lambda[\Gamma'_T]\lambda[\Gamma_T]\lambda[\Gamma_T]}\\
& \times\begin{pmatrix}\Gamma'_J & \Gamma'_V & \Gamma'_T\\ \gamma'_J & \gamma'_V & \gamma'^{*}_T\end{pmatrix}\begin{pmatrix}\hat{\Gamma}_J & \hat{\Gamma}_V & \hat{\Gamma}_T\\ \hat{\gamma}_J & \hat{\gamma}_V & \hat{\gamma}^{*}_T\end{pmatrix}\begin{pmatrix}\Gamma_J & \Gamma_V & \Gamma_T\\ \gamma_J & \gamma_V & \gamma^{*}_T\end{pmatrix}\\
& \times\begin{pmatrix}J' & V' & T'\\ \Gamma'_J & \Gamma'_V & \Gamma'_T\end{pmatrix}\begin{pmatrix}\hat{J} & \hat{V} & \hat{T}\\ \hat{\Gamma}_J & \hat{\Gamma}_V & \hat{\Gamma}_T\end{pmatrix}\begin{pmatrix}J & V & T\\ \Gamma_J & \Gamma_V & \Gamma_T\end{pmatrix}\\
& \times(-1)^{J(\Gamma'_J)+\gamma'^{*}_J}\cdot(-1)^{J(\Gamma'_V)+\gamma'^{*}_V}\begin{pmatrix}\Gamma'_J & \hat{\Gamma}_J & \Gamma_J\\ \gamma'^{*}_J & \hat{\gamma}_J & \gamma_J\end{pmatrix}\\
& \times\begin{pmatrix}J' & \hat{J} & J\\ \Gamma'_J & \hat{\Gamma}_J & \Gamma_J\end{pmatrix}\begin{pmatrix}\Gamma'_V & \hat{\Gamma}_V & \Gamma_V\\ \gamma'^{*}_V & \hat{\gamma}_V & \gamma_V\end{pmatrix}\begin{pmatrix}V' & \hat{V} & V\\ \Gamma'_V & \hat{\Gamma}_V & \Gamma_V\end{pmatrix}\\
& \times\langle J'||\hat{J}||J\rangle\langle V'||\hat{V}||V\rangle
\end{aligned}
\tag{31}
$$

with this expansion, the techniques for predicting the absorption, Raman, MCD, and emission spectra of vibronic systems and the radiationless vibronic transitions associated with the selection rule aspect of the golden rule have been constructed.

The transition moment itself is usually factored as a series of progressively weaker multipole contributions of which the monopole, dipole, quadrupole, and octapole are the first four terms. The monopole does not contribute to transitions for either electronic or vibrational processes because it implies a change in the metric of the displacement space being used. For electronic processes the first contributing term becomes the dipole. This moment is allowed because the separation of charge into a dipole does not shift the centre of charge with respect to the whole molecule. The motion is however ungerade and maps onto translation of an uncharged body for the purpose of assigning a point group representation.

In contrast, for vibrational processes the dipole may not contribute to internal transitions of mass motion. As just mentioned, the dipole corresponds to a shift of the centre of mass of uncharged particles, often called Bosons, and such motions are eliminated from the assignment of molecular normal modes by the $3N-6$ degrees-of-freedom rule. The quadrupole moment operator is forbidden, as it is in electronic cases, since the exciting photon is ungerade in character. Thus the first contributing term of the multipole expansion which satisfies all criteria for mass motion excitation is the octapole. The conclusion is not unique to molecular assemblies but is a well-known result for the interaction of gamma-ray photons with atomic nuclei [89]. (It is just one more debt theoretical chemistry must owe to prior developments by physicists.) In the case of even–even nuclei, the photon interacts essentially with a Boson array for which, as described above, the monopole and dipole processes are forbidden. The observable nuclear spectra fall into a strong octapole sequence and a moderately intense quadrupole spectrum which, like Raman processes in molecules, arises through second-order coupling.

This analogy between molecular mass and nuclear mass excitation processes can be used further to provide the identity of the infinite group for vibrations and the appropriate set of representation bases $|Vv\rangle$ [12] which appear in eqns. (29)–(31). The spherical nucleus requires the point group which describes harmonic motion in three dimensions. This group is the special unitary group in three dimensions SU(3) which contains as subgroups R_3 and all the finite groups of interest. Therefore, the subduction of finite group representations $|\Gamma_V\gamma_V\rangle$ from the infinite group employs the same projection algebra as the subduction of electronic bases [87]. There is a powerful formal economy in this parallel. Having identified the generative vibrational group, the generative group for the total vector can be found. We recall that the minimum generative group for the electronic bases is SU(2). By direct multiplication of this electronic momentum space with the nuclear momentum space SU(3), the total generative group becomes SU(6). In this six-dimensional group the electronic and vibrational bases remain uncoupled. The desired coupling of these vectors is achieved by restriction to a subspace in which only the coupled vector is well defined. By analogy with the techniques used to generate the spin–orbit coupled momentum $|JM_J\rangle$ from orbital $|LM_L\rangle$ and spin $|SM_S\rangle$, we wish to restrict SU(6) to a three-dimensional diagonal subgroup. This cannot be done directly since SU(6) cannot be written as a square matrix. We may however regard SU(2) as a subgroup of SU(3) for the electronic vectors and hence select the diagonal subgroup out of the product group $\mathrm{SU}(3) \times \mathrm{SU}(3) \in \mathrm{SU}(9)$. Thus the required generative group for the total representation T of vibronic coupling is SU(3).

This identification of the generative group of the total vector makes it possible to specify the selection rules of the coupled event. The more stringent of the two factored transition moment requirements is the octapole rule on the vibrational term. This limitation requires in turn that the overall operator must have at least octapole character. Hence allowed vibronic transitions occur only if

$$\hat{T} = 3 \quad (\text{in SU(3)})$$

and by subduction onto O_h for example

$$\hat{\Gamma} = T_{1u} \quad (\text{in } O_h)$$

As with the uncoupling of total basis functions, it is clear from eqn. (30) that this set of total conditions can result from the sum of any appropriate pair of $|\hat{J}\hat{\Gamma}_J\hat{\gamma}_J|$ and $|\hat{V}\hat{\Gamma}_V\hat{\gamma}_V|$. In most cases one term in this sum is dominant and typically arises from one of the following combinations of moments which may be observed:

Change in basis	$\lvert\Delta V\rvert$	$\lvert\Delta V\rvert$	$\lvert\Delta T\rvert$
Moment	Monopole	Octapole	Octapole
	Dipole	Quadrupole	Octapole
	Quadrupole	Dipole	Octapole
	Octapole	Monopole	Octapole

so that in every case the sum of the changes in basis functions is constant,

$$|\Delta J| + |\Delta V| = |\Delta T| = 3. \tag{32}$$

The same formalism applies to rovibrational couplings once it is recognized that the generative rotational group is SU(2) and that the rotation operator is hexadecapolar, $\hat{R} = 4$, and subduces onto $\hat{\Gamma}_R = T_{1g}$ in O_h.

This factorization procedure and the accompanying selection rules incorporate a restatement of the Franck–Condon principle in a new, analytic form. The conventional Franck–Condon expansion is the product of a "matrix element" for the normal mode displacement operator with a vibrational "overlap factor". This product correlates directly to the product in eqn. (31) of the Wigner–Eckart 3Γ symbol and the reduced matrix element for vibration. In particular, the Franck–Condon "matrix element" serves exactly the same purpose as the selection rules expressed in the 3Γ symbol for vibrational representations and components, and the "overlap integral" expresses the same magnitude of the effect as does the vibrational reduced matrix element. Our new expression however provides two advantages. It achieves a quantitative calculation of the magnitude since we can evaluate every term in eqn. (32) and it shows very clearly that the promoting mode in the "matrix element" (the 3Γ symbol) must be identical to the progression mode in the "overlap factor" (vibrational reduced matrix element). The two modes can no longer be considered as independent and in all levels of approximation the "overlap factors" can only be related to the modes permitted by the moment operator in question. This selection process includes in particular the totally symmetric mode which, like all other normal modes, can only contribute to a progression or coupling when permitted within both the finite and infinite group selection rules. In most cases, combination of this mode with others is forbidden by the selection rules in the infinite group.

Thus far, the selection rules have applied to the coupling of the electronic states with the first vibrational quantum. Since the vibronic transition octapole is ungerade in character, an allowed transition occurs only when one vector changes $(g \rightarrow u)$ or $(u \rightarrow g)$ while the other remains constant $(g \rightarrow g)$ or $(u \rightarrow u)$. This results in two distinct types of vibronic progression in point groups having sufficient symmetry to define a horizontal plane. For Laporte-allowed electronic transitions the vibrational quanta remain $(g \rightarrow g)$ assuming that no hot bands appear. Thus the successive vibronic intensities in this situation would reflect only the magnitudes of successive vibrational reduced matrix elements.

In contrast, Laporte-forbidden electronic origins require coupling of gerade electronic excited states to ungerade normal modes in the absence of hot bands. However the even overtones of ungerade modes are gerade and hence the even transitions in the vibronic progression are forbidden under the octapole operator. This forbiddenness can be broken in second order by any molecular motions which destroy centres of symmetry but the successive intensities in the vibronic progression will be characterized by an alternation superimposed upon the envelope of vibrational reduced matrix elements. The observation of an alternation on a Laporte-forbidden transition is therefore an indication of first-order coupling to an ungerade normal mode (Fig. 6).

(iii) Derivation of first-order photochemical reaction coordinates

All of the individual steps which can be envisioned as part of an overall photoevent can be analysed with these tensorial techniques. Beyond this analysis of separate processes, however, the tensor component (vector) coupling formalism provides a new basis for constructing the reaction surfaces themselves. In the conventional model, the Born–Oppenheimer approximation provides the crucial separation of electronic and vibrational terms. By assuming further that reaction energies are predominantly determined by the electronic state energies, a set of continuous surfaces relating state energies to relative nuclear positions can be derived. The smaller effects of the weakly coupled vibrations are then included as quantized levels within the available minima. As described above however, it is not necessary to use the severe limitations imposed by the Born–Oppenheimer approximation to achieve the desired separation of variables.

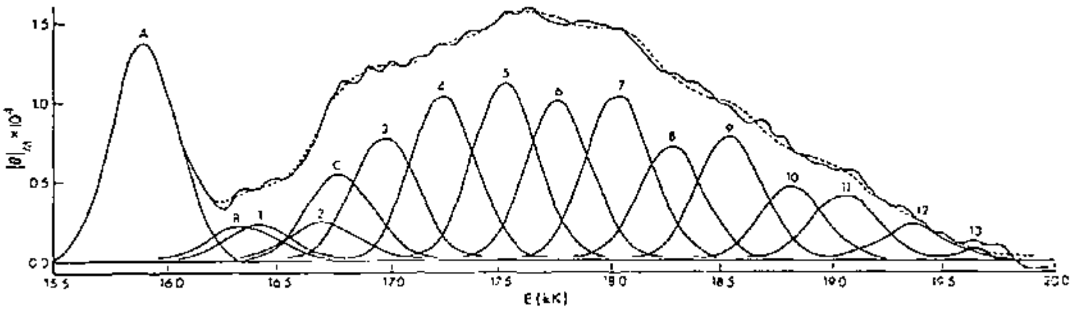

Fig. 6. First-order coupling to an ungerade normal mode shown in the spectrum of $Cr(OH_2)_6^{3+}$.

The same mathematical convenience is obtained through the vector decoupling procedure without any assumptions concerning the vibronic coupling strength.

Once the reaction surfaces have been prepared, photo and decay processes are usually regarded as instantaneous vertical events between surfaces. The transition moment calculations, by either conventional or tensor techniques, define the probabilities of each event to any desired order of approximation. The tensorial approach makes it clear however, that a very limited number of vibronic coupling channels are available in most promotion and decay processes. Since the promoting and progression modes must be identical for any particular order of approximation, many anticipated "holes" or "funnels" for decay between surfaces at avoided crossings [81] may in fact be strongly forbidden. In other words, the probabilities for decay channels in particular, will not depend exclusively on the inverse energy gap rule, but in addition, on well-defined selection rules.

The ultimate test of any model, including the tensorial view of photo and decay processes just described, is its ability to predict and correlate observable events. However, the selection rules which are derived here are "first order". Obviously, if all processes are first-order forbidden, it becomes worthwhile to start examining second-order terms. Practically speaking, this means that the present analysis is most likely to make valid predictions for behaviour of DOSENCO states where first-order allowed terms lead to observed rates, r_{obs}, which approach within one to three orders of magnitude of r_{fund} of eqn. (26). When r_{obs} is less, there is a much greater chance that the system "discovers" first-order forbidden paths which become partially allowed in higher order. However, it is worth noting that the slower processes are the ones most effectively treated by the theory and mechanistic analysis of DERCOS states borrowed from thermal kinetics. The area of most urgent need for new theory is precisely the area of prompt processes with r_{obs} approaching r_{fund}.

We therefore make the one major assumption that the reactions of DOSENCO states will occur along the reaction coordinate determined by the first-order vibronic coupling. Based on the tensor analysis of vibronic coupling in eqns. (31) and (33), a general procedure for identifying this potentially photoreactive coordinate can be formulated.

(a) Assume that the vibronic intensity and hence probability of the reaction coordinate is governed by an overall octapole rule, $|\Delta T| = 3$.

(b) Assume that this rule can be factored into sums of absolute changes of electronic and vibrational angular momentum following eqn. (33)

$$|\Delta J| + |\Delta V| = |\Delta L| + |\Delta S| + |\Delta V| = |\Delta T| = 3.$$

(c) Define the changes in orbital $|\Delta L|$ and spin $|\Delta S|$ momenta in transition metal complex spectra from an intermediate ligand field fit of the experimental data [84,85].

(d) Substitute these known values into eqn. (33) and arrange to define the vibrational momentum change

$$\begin{aligned} |\Delta V| &= |\Delta T| - [|\Delta L| + |\Delta S|] \\ &= 3 - [|\Delta L| + |\Delta S|] \end{aligned}$$

Note that $|\Delta L|$ is calculated on a modulus of 4 [87] as discussed in detail below.

(e) Assume the vibrational momentum of the ground state is zero ($V = 0$) and associate $|\Delta V|$ with the appropriate projected octahedral normal mode (Fig. 7). (Exclude "hot ground state" processes.)

(f) In the assignment of normal modes from any $|\Delta V|$ use only those which have non-vanishing amplitude at the ligands.

(iv) Prediction of behaviour of DOSENCO states

As a case of particular interest in inorganic photochemistry, the vibrational modes accompanying the ligand field transitions in octahedral d^3 complexes can be predicted. Thus from eqn. (33), if $|\Delta T|$ must always be 3

	$\|\Delta J\|$		$\|\Delta V\|$
$^4A_{2g}(F) \leftrightarrow {}^4(T_{2g})(F)$	0	then	3
or			
$^4A_{2g}(F) \leftrightarrow {}^2T_{1g}(G)$	2	then	1
or			
$^4A_{2g}(F) \leftrightarrow {}^2E_g(G)$	2	then	1

where $|\Delta J| = |\Delta L| + |\Delta S|$. If the ground-state vibration is $|0a_{1g}\rangle$, then the $^4T_{2g}(F)$ state can couple with normal modes subduced from $V = 3$ which

Octahedral Normal Modes

and Their Basis Functions

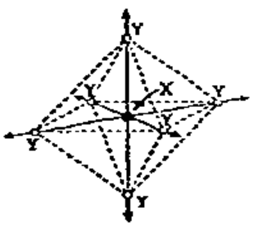

ν_1

$|0a_{1g}0\rangle = |00\rangle$

Breathing

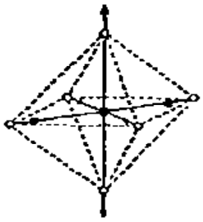

ν_2

$|2e_g0\rangle = |20\rangle$

Symmetric Stretch

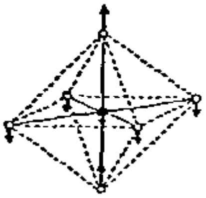

ν_4

$|1t_{1u}0\rangle = |10\rangle$

Asymmetric Stretch

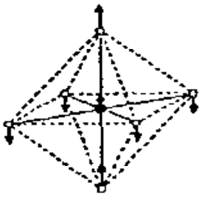

ν_3

$|3t_{1u}0\rangle = |30\rangle$

Buckle

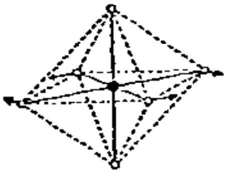

ν_5

$|2t_{2g}0\rangle = \frac{1}{\sqrt{2}}(-|22\rangle + |2\text{-}2\rangle)$

Wag

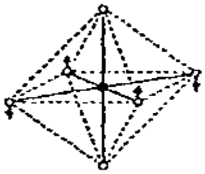

ν_6

$|3t_{2u}0\rangle = \frac{1}{\sqrt{2}}(|32\rangle + |3\text{-}2\rangle)$

Twist

Fig. 7. Octahedral normal modes and their basis functions.

have non-vanishing probabilities at the ligands. The only mode fulfilling both these requirements is the $|3t_{1u}\rangle$ buckle (Fig. 7). The t_{2u} corresponds to a normal mode with nodes at the ligand and hence cannot couple in first order to the electronic vector. Similarly the ${}^2T_{1g}$ and ${}^2E_g$ states can only couple with normal modes from $V=1$ which do not vanish at the ligands. Again the only mode is t_{1u} but now $|1t_{1u}\rangle$ represents an antisymmetric stretch. The two t_{1u} modes are completely orthogonal by virtue of their different generative group derivations. Recent MCD spectroscopic analysis of the ${}^4T_{2g}$ and ${}^2T_{1g}$ bands in $[Cr(H_2O)_6]^{3+}$ in aqueous solution gives no evidence at all that these two t_{1u} modes mix, although the progressions overlap extensively [12].

The tensorial model developed thus far predicts therefore that excitation of the ${}^4T_{2g}(F)$ state is rapidly accompanied by the t_{1u} buckle motion (Fig. 7). If this motion is violent enough, it could expose the metal on stretched faces of the octahedral complex. On compressed faces, the equatorial ligands could interact sterically with the apical ligand and result in rearrangements in the first coordination sphere. Such pathology of the DOSENCO state could thus lead to very rapid associative ligand replacement reactions or, if no replacement of ligands were involved, to racemization or pseudo-rotation between isomeric species.

Excitation of the ${}^2T_{1g}(G)$ state on the other hand, rapidly leads to antisymmetric stretching along metal–ligand bonds. If this becomes pathological, it would lead initially to ligand dissociation and formation of a five-coordinate intermediate which could react either by recombination or acquisition of a replacement from the second-coordination sphere. The quantum yields of these two specific chemical channels in the same chemical environment will depend on the restoring force of the vibrational mode in the particular excited overtone. While this is difficult to predict in particular, the antisymmetric stretch usually has a substantially larger restoring force than the buckle mode, so that in first order, states coupled to the latter mode should result more easily in chemical change.

As in the case of d^3 systems, the reaction coordinates for specific events of photoexcited d^6 systems can be predicted using the general rules. Thus for transitions observed in the visible region in six-coordinate Co(III) complexes

	ΔJ		ΔV
${}^1A_{1g}({}^1I) \rightarrow {}^5T_{2g}({}^5D)$	2	then	1
${}^1A_{1g}({}^1I) \rightarrow {}^3T_{1g}({}^3H)$	2	then	1
${}^1A_{1g}({}^1I) \rightarrow {}^3T_{2g}({}^3H)$	2	then	1
${}^1A_{1g}({}^1I) \rightarrow {}^1T_{1g}({}^1I)$	0	then	3

We note here, as mentioned in the general rules, that the effective $\Delta J = 2$ in the first case while the actual ΔJ is the sum of $|\Delta L| = 4$ and $|\Delta S| = 2$ for a total of 6. In the derivation of the octahedral Hamiltonian for d electrons however, a closed algebra in L is defined by the four-fold axis of symmetry. Therefore the maximum change in L is 3, and $|\Delta L| = 4$ maps directly onto $|\Delta L| = 0$. In the present case therefore, the effective $|\Delta J| = 2$ [87]. Assuming as usual that the ground state vibration is $|0a_{1g}\rangle$, then all states involving a spin change are promoted by the asymmetric stretch while the singlet–singlet transition, as in d^3 systems, carries the buckle motion.

In the preceding paragraphs, the detailed analysis of d^3 and d^6 excited states has been given because the well-characterized examples are all from these configurations. However there are many other classes of compounds for which equally detailed and useful predictions of behaviour can be made. The most intense transitions in ligand field spectra are spin allowed and often arise from free ion configuration for which $|\Delta L| = 0$. Thus ligand field spectra and photochemistry often illustrate the first case in eqn. (33). The second case, $\Delta J = 1$, $\Delta V = 2$, $\Gamma_V = e_g$ is often seen in aromatic compounds. For example the absorption spectrum of the dipole allowed $\pi \rightarrow \pi^*$ transition origin in phthalocyanines is accompanied by a progression, identified from MCD analysis, of non-degenerate vibronic states [90]. These can only arise from the predicted coupling of a quadrupole e_g vibration with the dipole ^1E_u state. The third case, $\Delta J = 2$, $\Delta V = 1$, $\Gamma_V = t_{1u}$, is illustrated by the Judd–Offelt effect in rare earth complexes [91] and by the Raman spectra of phthalocyanines [92] in which only the dipole allowed vibrations are observed. The last case, $\Delta J = 3$, $\Delta V = 0$, $\Gamma_V = a_{1g}$, has been identified during work in progress [88] on the spectrum of benzene in which the predicted totally-symmetric vibrational mode is clearly the dominant feature of the observed electronic octapole band.

(v) Comparison of predicted and observed DOSENCO state behaviour

DOSENCO state processes or DERCOS state processes for quite short-lived DERCOS states are associated with "octahedral photosubstitution" at Cr(III), Co(III), Rh(III), and d^6 M(CO)$_6$ centres. The most obvious prediction from the theoretical selection rules is stereochemical. From the foregoing discussion, reaction involving the buckle mode of the octahedra in coupled excited states is expected to result in facile isomerization. Reactions involving the asymmetric stretching mode, on the other hand, are expected to proceed with stereochemical retention.

The general rules show that the Cr(III) quartet states couple to the $|3t_{1u}\rangle$ vibration in first order. This provides an immediate explanation for the widespread occurrence of stereoisomerization in Cr(III) reactions. It also explains the very low quantum yield for *trans*-Cr(cyclam)Cl_2^+ [93]. One Cr(III) complex, $Cr(bpy)_3^{3+}$ has been shown to react from the ^2E excited state. In this case, our analysis requires coupling to quartet ground states via the $|1t_{1u}\rangle$ stretch in first order. Despite the fact that the lifetime of the ^2E state of this complex is microseconds, and first-order forbidden processes may be involved in its relaxation, the substitution product is probably *cis*-$Cr(bipy)_2(OH)_2^+$ [22] (which may prove very little).

The behaviour of d^6Rh(III) complexes has been discussed earlier. Substitution is stereoretentive and *trans*-Rh(cyclam)Cl_2^+ is reactive [35]. This is consistent with assignment of reactions to the ligand field triplet which couples to singlet ground states via the asymmetric stretch. The corresponding d^6Co(III) complexes are a little less unambiguous. It is not certain which excited state is precursor to reaction. It may be $^3T_1$ as in the Rh(III) case or it may be that $^5T_2$ is involved in these weaker field systems as has been suggested from both experiment [94] and theory [95]. In either case, our analysis suggests a coupling to singlet ground states through the asymmetric stretch. This means stereoretention should dominate. It is clear that stereoretention is vastly more common than in corresponding Cr(III) reactions [68]. It is quite interesting that the stereoisomerization, which is observed in the case of aquation of *cis*-$Co(en)_2(NH_3)Cl^{2+}$, is attributed by Pribush et al. [74] to an edge displacement by an initially activated coordination position of ethylenediamine. This would assign the isomerization to a post-photo, DERCOS, process or a highly reactive intermediate.

Another case is $M(CO)_6$ (M = Cr, Mo, or W). Here, the primary photoproduct, $M(CO)_5$, has been the subject of extensive investigation in low-temperature matrices [47]. There is production of the trigonal bipyramid D_{3h} form of $M(CO)_5$ but it seems nearly certain that this is the product of thermal DERCOS isomerization of the primary photoproduct, $C_{4v}M(CO)_5$. The C_{4v} product is the predicted product from the triplet which is clearly indicated to be the photoreactive state.

To illustrate the scope of the theory the final example considered will draw on different and much less straightforward experimental data. This case draws attention to the importance of a capacity to understand medium effects. The first-order selection rules do give an indication of factors involved in intersystem crossing processes. Consider relaxation of ^2E_g states of *trans*-$Cr(NH_3)_2(NCS)_4^-$ to a $^4A_{2g}$ ground state (approximate O_h symmetry — $^4A_{2g}$ is either a product state or the original ground state). The rate of this relaxation is medium dependent [32] as was noted in Section C(iii). The medium must provide a quadrupole in order to couple these states. This is because it requires a quadrupole operator to couple the asymmetric stretch mode to the asymmetric buckle mode and this coupling is seen spectroscopically to be involved in the $^2E \leftarrow {}^4A_{2g}$ transition. The thermal substitution reaction of *trans*-$Cr(NH_3)_2(NCS)_4^-$ is quite sensitive to deuteration of the amine ligands. This was attributed to the role of H-bonding from the N–H moiety to the solvent [93]. Selection of *trans* solvent molecules for strong interaction would be the simplest way to gain a quadrupole interaction with the medium. The medium dependence of ^2E phosphorescence lifetimes of this complex can be understood from this point of view. Fastest relaxation occurs in water and other hydroxylic solvents. Good H-bond acceptors which are rather large molecules (and subject to some steric crowding limits) are intermediate. The longest lifetimes are associated with poor H-bond acceptors like CH_3CN and CH_2Cl_2.

Thus, conclusions need not be limited to prediction of photochemistry alone but can be applied equally to predict the probabilities of competing photophysical processes. Those of greatest concern include the various types of emission and the radiationless processes which promote internal conversion or intersystem crossing. In all cases the transition moment operator must first be identified. Those normally used for spontaneous emission prediction are the same as described earlier for absorption and need not be discussed further. The operators needed for radiationless processes however are poorly understood, and as a result most predictive attempts to date have relied heavily on statistical models concerning probabilities of overlap of excited molecular states with densities of states in the heat bath. In fact, this situation is strongly reminiscent of the Franck–Condon treatment of absorption-emission vibronic transitions. However, before we attempt to convert the golden rule for radiationless processes to the tensor form the physical nature of the connection between excited molecular states and the heat bath must be made more explicit. Perhaps our best clue arises from the earlier discussion of DOSENCO states. The buckle mode was predicted to be more active photochemically than the antisymmetric stretch because of its lower restoring force or, in other words, its greater excursion from equilibrium. By the same argument the buckle mode and other angular deflection modes should also interact more effectively with the molecules of the heat bath. The most effective operator for radiationless transitions therefore is probably a sum of the available angular distortion modes of the electronically excited molecule.

If we assume, as have the earlier statistical treatments, that the density of heat bath rovibrational states is high, then these angular deflection modes will always have significant overlap with "group normal modes" of the heat bath with the appropriate symmetry. Indeed, the coupling to the bath is not usually considered to be the rate determining step in radiationless transition rates. The rate will be determined chiefly by the initially excited mode. If, as in the $^4T_{2g}$ excitation, an angular deflection mode is directly excited, we can expect radiationless rates to be high whereas, as in the $^2T_{1g}$ excitation, the coupling to a stretch mode should lead to long excited state lifetimes. Thus the predicted rapid decay of the $^4T_{2g}(F)$ state either by DOSENCO chemical or physical relaxation channels is a function of the initial excitation process. The model predicts, as well, the high activation barriers to specific channels for the $^2T_{1g}(G)$ state. It cannot directly predict the eventual decay route after thermal equilibrium of the latter state is achieved, a problem better approached through our earlier discussion of thermally mitigated processes.

ACKNOWLEDGEMENTS

We thank Dr. Willem Siebrand for valuable discussions, Dr. J.I. Zink for access to unpublished calculations, and Dr. A.D. Kirk for results prior to publication. Our work is supported by the Natural Sciences and Engineering Research Council (Canada).

REFERENCES

1 C.H. Langford and B.R. Hollebone, IUPAC Coord. Chem., 20 (1980) 57.
2 V. Balzani, F. Bolletta, M.T. Gandolfi and M. Maestri, Top. Curr. Chem., 75 (1978) 1.
3 M.A. Jamieson, N. Serpone and M.Z. Hoffman, Coord. Chem. Rev., 39 (1981) 121.
4 For a review see: E. Zinato, in A.W. Adamson and P. Fleischaur (Eds.), Concepts in Inorganic Photochemistry. Wiley-Interscience, New York, 1975, Chap. 4.
5 A.W. Adamson, Pure Appl. Chem., 24 (1970) 451.
6 P.C. Fleischaur, A.W. Adamson and G. Sartori, Prog. Inorg. Chem., 17 (1972) 1.
7 G.S. Hammond, Adv. Photochem., 7 (1969) 373.
8 L.G. Vanquickenborne and A. Ceulemans, J. Am. Chem. Soc., 99 (1977) 2208.
9 L.G. Vanquickenborne and A. Ceulemans, J. Am. Chem. Soc., 100 (1978) 475.
10 L.G. Vanquickenborne and A. Ceulemans, Inorg. Chem., 18 (1979) 3475.
11 K.F. Freed, Acc. Chem. Res., 11 (1978) 74.
12 B.R. Hollebone, Theor. Chim. Acta, 56 (1980) 45.
13 A.W. Adamson, R.C. Fukuda, M. Larson, M. Macke and J.P. Piraux, Inorg. Chim. Acta Lett., 44 (1980) 113.
14 G.S. Hammond, J. Am. Chem. Soc., 77 (1955) 334.
15 A.D. Kirk, P.E. Hoggard, G.B. Porter, M.G. Rockley and M.W. Windsor, Chem. Phys. Lett., 37 (1976) 199.
16 J.A. Koningstein, personal communication, 1980.
17 R.A. Marcus, Annu. Rev. Phys. Chem., 15 (1966) 155.
18 W.J. Albery, Annu. Rev. Phys. Chem., 29 (1980) 230.
19 Z.R. Grabowski and W. Rubaszewska, J. Chem. Soc., Faraday Trans., 73 (1977) 11.
20 R. Ballardini, G. Varani and V. Balzani, in press.
21 M. Maestri, F. Bolletta, L. Moggi, V. Balzani, M.S. Henry and M.Z. Hoffman, J. Am. Chem. Soc., 100 (1978) 2694.
22 M.A. Jamieson, N. Serpone, M.S. Henry and M.Z. Hoffman, Inorg. Chem., 18 (1979) 214.
23 R. Sriram, M.S. Henry and M.Z. Hoffman, Inorg. Chem., 18 (1979) 1727.
24 F. Bolletta, M. Maestri and V. Balzani, J. Phys. Chem., 80 (1979) 2499.

25 M.A. Jamieson, N. Serpone and M. Maestri, Inorg. Chem., 17 (1978) 2432.
26 R.L.P. Sasseville and C.H. Langford, Inorg. Chem., in press.
27 N. Sutin, J. Photochem., 10 (1979) 19.
28 T.W. Swaddle, Coord. Chem. Rev., 14 (1974) 217.
29 A.R. Gutierrez and A.W. Adamson, J. Phys. Chem., 82 (1978) 902.
30 N.A.P. Kane-Maguire, G.M. Clonts and R.C. Keir, Inorg. Chim. Acta, 44 (1980) 1157.
31 For a review see: P.C. Ford, R.E. Hintze and J.D. Petersen, ref. 4, Chap. 5.
32 M.A. Bergkamp, R.J. Watts, P.C. Ford, J. Brannon and D. Magde, Chem. Phys. Lett., 59 (1978) 125.
33 M.A. Bergkamp, J. Brannon, D. Magde, R.J. Watts and P.C. Ford, J. Am. Chem. Soc., 101 (1979) 4549.
34 R.T. Walters and A.W. Adamson, Acta Chem. Scand., A33 (1979) 53.
35 R. Rumfeldt and J. Sellan, Can. J. Chem., 54 (1976) 519,1061.
36 C.M. Owens, Ph.D. Thesis, University of Windsor, Canada, 1978.
37 R. Rumfeldt, private communication, 1980.
38 J.I. Zink, J. Am. Chem. Soc., 96 (1974) 4464.
39 J.I. Zink, J. Am. Chem. Soc., 94 (1972) 8039.
40 J.I. Zink, Inorg. Chem., 12 (1973) 1018.
41 H. Okabe, The Photochemistry of Small Molecules. Wiley, New York, 1978, Chap. II.
42 H. Okabe, J. Chem. Phys., 66 (1977) 2–58.
43 H. Franck and E. Rabinowitsch, Trans. Faraday Soc., 30 (1934) 120.
44 A. Harriman, Coord. Chem. Rev., 28 (1979) 147.
45 J. Zimmerman, J. Chem. Phys., 23 (1955) 825.
46 C.E. Wulfman, Dynamical Groups in Atomic and Molecular Physics, in J.C. Donini (Ed.), Advances in Group Theory and their Application to Spectroscopy. Plenum, New York, 1979.
47 G.L. Geoffrey and M.S. Wrighton, Organometallic Photochemistry. Academic Press, New York, 1979, Chap. III.
48 A.J. Rest and J.R. Sodeau, J. Chem. Soc., Faraday Trans. 1, 74 (1978) 1691.
49 W. Strohmeier and D. van Hobe, Z. Phys. Chem. (Frankfurt am Main) 34 (1962) 393.
50 M. Wrighton, G.S. Hammond and H.B. Gray, Mol. Photochem., 5 (1973) 179.
51 G. Swenzer, M.Y. Darensbourg and D.J. Darensbourg, Inorg. Chem., 11 (1972) 1967.
52 S.N. Chen and G.B. Porter, Chem. Phys. Lett., 6 (1970) 41.
53 N.A.P. Kane-Maguire and C.H. Langford, J. Chem. Soc., Chem. Commun., (1973) 351.
54 C.H. Langford and L. Tipping, Can. J. Chem., 50 (1972) 887.
55 R. Ballardini, G. Varani, H.F. Wasgestian, L. Moggi and V. Balzani, J. Phys. Chem., 77 (1973) 2974.
56 N.A.P. Kane-Maguire and C.H. Langford, J. Am. Chem. Soc., 94 (1972) 2125.
57 H.F. Wasgestian, J. Phys. Chem., 76 (1972) 1947.
58 N.A.P. Kane-Maguire, J.E. Phifer and C.J. Toney, Inorg. Chem., 15 (1976) 593.
59 S.C. Pike and M.W. Windsor, J. Am. Chem. Soc., 100 (1978) 6518.
60 C.H. Langford, R. LeSage and R.W. Yip, Abstracts National Meeting, Chemical Institute of Canada, Ottawa, June 1–4, 1980.
61 D. Sandrini, M.T. Gandolfi, L. Moggi and V. Balzani, J. Am. Chem. Soc., 100 (1978) 1463.
62 M.T. Gandolfi, F.E. Manfrin, A. Juris, L. Moggi and V. Balzani, Inorg. Chem., 13 (1974) 1342.
63 C.F.C. Wong and A.D. Kirk, Inorg. Chem., 15 (1976) 1519.
64 W.J. Rosebush and A.D. Kirk, Can. J. Chem., 54 (1976) 2335.

65 A.D. Kirk and C.F.C. Wong, Inorg. Chem., 18 (1979) 593.
66 A.D. Kirk, private communication, 1980.
67 C.H. Langford and R.L.P. Sasseville, J. Am. Chem. Soc., 101 (1979) 5834.
68 R.A. Pribush, C.K. Poon, C.M. Bruce and A.W. Adamson, J. Am. Chem. Soc., 96 (1974) 3027.
69 P.S. Sheridan and A.W. Adamson, J. Am. Chem. Soc., 96 (1974) 3032.
70 J.F. Endicott, G.J. Ferraudi and J.R. Barber, J. Phys. Chem., 79 (1975) 630.
71 J.F. Endicott and T.L. Netzel, J. Am. Chem. Soc., 101 (1979) 4000.
72 G.J. Ferraudi, J.F. Endicott and J.R. Barber, J. Am. Chem. Soc., 97 (1975) 6406.
73 C.H. Langford and C.P.J. Vuik, J. Am. Chem. Soc., 98 (1976) 5409.
74 R.A. Pribush, R.E. Wright and A.W. Adamson, J. Am. Chem. Soc., 99 (1977) 2495.
75 A. Devaquet, J. Am. Chem. Soc., 94 (1971) 5626, 9102.
76 H. Yersim, H. Oho, J.I. Zink and G. Glieman, J. Am. Chem. Soc., 102 (1980) 951.
77 R.B. Woodward and R. Hoffman, Angew. Chem. Int. Ed. Engl., 8 (1969) 781.
78 H.C. Longuet-Higgins and E.W. Abrahamson, J. Am. Chem. Soc., 87 (1965) 2045.
79 A.D. Kirk and C.F.C. Wong, Inorg. Chem., 18 (1979) 593.
80 J.I. Zink, personal communication, 1979.
81 N.J. Turro, Modern Molecular Photochemistry. Benjamin-Cummings, New York, 1978.
82 W. Kauzman, Quantum Chemistry. Academic Press, New York, 1957, pp. 532, 664.
83 S. Nordholm and S.A. Rice, J. Chem. Phys., 62 (1975) 157.
84 J.C. Donini, B.R. Hollebone and A.B.P. Lever, Prog. Inorg. Chem., 22 (1977) 225.
85 J.C. Donini and B.R. Hollebone, Theor. Chim. Acta, 42 (1976) 111.
86 P.H. Butler, Properties and Application of Point Group Coupling Coefficients, in J.C. Donini (Ed.), Advances in Group Theory and their Application to Spectroscopy. Plenum, New York, 1979.
87 B.R. Hollebone and J.C. Donini, Theor. Chim. Acta, 42 (1976) 97.
88 B.R. Hollebone, W. Siebrand and J.C. Donini, private communication, 1980.
89 J.M. Irvine, Nuclear Structure Theory. Oxford University Press, Oxford, 1972.
90 B.R. Hollebone and M.J. Stillman, J. Chem. Soc., Faraday Trans. 2, 74 (1978) 2107.
91 B.R. Hollebone and M.J. Stillman, Chem. Phys. Lett., 66 (1979) 248.
92 W. Siebrand and M.Z. Zgierski, in E.C. Lim (Ed.), Excited States, 4 (1980).
93 N.A.P. Kane-Maguire, J. Conway and C.H. Langford, Chem. Commun., (1974) 801.
94 V.S. Sastri, S. Behrendt, R.W. Henwood and C.H. Langford, J. Am. Chem. Soc., 94 (1972) 753.
95 R.B. Wilson and E.I. Solomon, J. Am. Chem. Soc., 102 (1980) 4085.